TITLE

Reactive Oxygen Detoxification Contributes to *Mycobacterium abscessus* Antibiotic Survival

AUTHORS

Nicholas A. Bates[1,2], Ronald Rodriguez[3,4], Rama Drwich[1], Abigail Ray[5], Sarah A. Stanley[3], Bennett H. Penn[1,6]*

AFFILIATIONS:

1. Department of Internal Medicine, University of California, Davis, California, USA
2. Graduate Group in Immunology, University of California, Davis, California, USA
3. Department of Molecular & Cell Biology, University of California, Berkeley, California, USA
4. Department of Plant & Microbial Biology, University of California, Berkeley, California, USA
5. Microbiology Graduate Group, University of California, Davis, California, USA
6. Department of Medical Microbiology and Immunology, University of California, Davis, California, USA

*Corresponding author

Email: bhpenn@ucdavis.edu

ABSTRACT

When a population of bacteria is exposed to a bactericidal antibiotic, most cells die rapidly. However, a sub-population of antibiotic-tolerant cells known as “persister cells” can survive for prolonged periods. In addition, antibiotic tolerance can be broadly induced throughout the population by stresses such as nutrient deprivation. However, the pathways required to maintain viability in this setting, and how stress induces antibiotic tolerance are both poorly understood. To identify genetic determinants of antibiotic tolerance in mycobacteria, we carried out transposon

mutagenesis insertion sequencing (Tn-Seq) screens in *Mycobacterium abscessus* (*Mabs*) exposed to bactericidal translation-inhibiting antibiotics. This analysis identified genes essential for the survival of both spontaneous persister cells as well as for stress-induced tolerance, allowing the first genetic comparison of these states in mycobacteria. Pathway analysis identified multiple genes involved in the detoxification of reactive oxygen species (ROS), including the catalase-peroxidase *katG*, which contributed to survival in both unstressed and nutrient-starved cells. In addition, we found that endogenous ROS were generated by translation-inhibiting antibiotics, and that hypoxia impaired bacterial killing. *KatG* specifically contributed to survival following exposure to transcription or translation inhibitors, but not other antibiotic classes tested. Thus, the lethality of some antibiotics is amplified by toxic ROS accumulation, and antibiotic-tolerant cells require detoxification systems to remain viable. These findings further demonstrate that antibiotic-induced ROS plays a broad role in mediating antibiotic lethality across diverse organisms.

INTRODUCTION

A key goal of antibiotic therapy is, in conjunction with the immune system, to eradicate the infecting bacteria. While many common bacterial infections respond rapidly to antibiotics, with 1-2 weeks of therapy sufficient to achieve high cure rates, there are also infections where bacterial clearance is slow and often incomplete[1, 2]. This challenge is exemplified by mycobacterial infections. Fully-susceptible *Mtb* requires multiple antibiotics for four months or longer[3], and infections by non-tuberculous mycobacteria (NTM), such as *Mycobacterium abscessus* (*Mabs*), are even more difficult to eradicate; *Mabs* often requires treatment for 12-18 months, and even then has a 50% relapse rate[4, 5].

While the ability of mycobacteria to escape antibiotic-mediated killing is multifactorial, the phenomenon of antibiotic tolerance is likely an important contributor[6-9]. Studies dating from the

53 1940s noted that when a population of susceptible bacteria were exposed to a bactericidal
54 antibiotic such as penicillin, the majority of the population died within a few hours, but that a small
55 sub-population of cells remained viable for days[10]. Importantly, these antibiotic-tolerant cells
56 referred to as "persister cells" had not acquired a mutation conferring heritable antibiotic
57 resistance, and do not grow in the presence of the antibiotic. Rather, they had entered into a
58 readily reversable phenotypic state where, despite antibiotic-mediated inhibition of critical
59 processes, they were able to survive[11-13]. In addition, a number of physiologic stresses increase
60 antibiotic tolerance in a population, as bacterial cell death is markedly slowed by stresses such
61 as nutrient deprivation or acidic pH[9, 10, 14, 15]. Notably, these same stresses are encountered in the
62 lysosome of an activated immune cell[16], and studies of pathogens isolated from activated
63 macrophages indeed show a strong immune-mediated increase antibiotic tolerance[8, 17]. Thus,
64 paradoxically, the immune system may actually impede bacterial eradication by antibiotics.
65
66 Antibiotic tolerance has been studied extensively in model systems such as *Escherichia coli*,
67 which has provided important insights, but also highlighted uncertainties of current paradigms.
68 Several different regulators of antibiotic tolerance have been identified in *E. coli* including the
69 HipBA toxin-antitoxin system[18], guanosine pentaphosphate ((p)ppGpp) synthesis by RelA/SpoT
70 enzymes [19-22], and Lon protease[23]. In each of these models, the postulated mechanism is to slow
71 metabolism or cell division and render the process targeted by antibiotics non-essential. However,
72 important questions remain. It is unclear how cells remain viable when critical processes, such as
73 transcription or translation, are blocked by antibiotics, as well as how antibiotic tolerance is
74 induced by stress. Even the mechanism of cell death following antibiotic exposure itself has been
75 a matter of debate - originally antibiotics were presumed to kill bacteria as a direct result of
76 inhibition of their target molecule, such as β-lactam antibiotics disrupting cell wall integrity, directly
77 leading to mechanical cell lysis[24]. However, a number of studies, largely from *E. coli*, have
78 demonstrated that in addition to the initial target inhibition, which may be bacteriostatic,

79 bactericidal antibiotics can also cause secondary lethal ROS accumulation, leading to cell death[13, 25-30].

81

82 Mycobacterial persister cells are particularly resilient, as *Mycobacterium smegmatis* (*Msmeg*) and
83 *Mycobacterium tuberculosis (Mtb)* persisters can endure many weeks of antibiotic exposure, and
84 stress-induced antibiotic tolerance develops readily[9, 13, 28]. *Mabs* is a species of rapidly-growing
85 mycobacteria, with a doubling time of ~4h in rich media[31], and while often environmental, it causes
86 opportunistic infections in patients with structural lung disease such as cystic fibrosis. It is also
87 among the most difficult of all bacterial pathogens to treat, because in addition to forming persister
88 cells, it is also intrinsically resistant to many classes of antibiotics, leaving few treatment options[5].
89 This leads to the use of antibiotics with greater toxicity to patients and a need to use these agents
90 for prolonged periods to prevent relapse. Thus, identifying the genes that *Mabs* persister cells rely
91 on for survival, as well as the genes involved in the induction and maintenance of stress-induced
92 antibiotic tolerance might highlight pathways that could be targeted therapeutically to eliminate
93 antibiotic-tolerant cells.

94

95 Previous genetic screens have studied antibiotic responses in mycobacteria, with some
96 evaluating heritable resistance, and others investigating tolerance. Several studies of resistance
97 have successfully used either transposon mutagenesis with insertion site sequencing (Tn-Seq)
98 or CRISPR-based transcriptional repression with high-throughput sequencing of guide RNAs
99 (CRISPRi) to identify genes promoting growth in sub-inhibitory concentrations of antibiotic. These
100 studies have provided insights, such as highlighting the importance of cell membrane permeability
101 as a mechanism controlling antibiotic penetration into the cytoplasm[32-34].

102

103 Persister formation has proven challenging to study, likely because the low frequency of persisters
104 leads to population bottlenecks that confound genetic analysis. Although screens in *Mtb* have been

105 conducted in macrophages and mice, and genes, such as *glpK* and *cinA* identified, overall the
106 number of mutants isolated in these screens has been low[35, 36]. There has been one effective in
107 vitro Tn-Seq study examining antibiotic tolerance in *Mtb* exposed to starvation and rifampin that
108 isolated over 100 mutants[29], demonstrating the feasibility of genetic screening in this context.
109 However, whether these phenotypes seen with rifampin in *Mtb* extend to other mycobacteria and
110 other antibiotics remains to be determined.
111
112 Here, we study antibiotic tolerance in *Mabs* and describe the results of genome-wide Tn-seq
113 screens seeking to identify the genes required for both spontaneous persister cell survival as well
114 as starvation-induced antibiotic tolerance following exposure to translation-inhibiting antibiotics.
115 We identified several discrete processes contributing to survival and observed a prominent role
116 for ROS detoxifying factors, such as the catalase-peroxidase enzyme KatG, which contributed to
117 both spontaneous persister survival and starvation-induced antibiotic tolerance. Consistent with
118 the protection conferred by KatG, we found that endogenous ROS accumulated following
119 antibiotic exposure, and that the removal of oxygen significantly impaired bacterial killing. Taken
120 together these findings support a model in mycobacteria where the lethality of translation-
121 inhibiting antibiotics is amplified by a secondary accumulation of toxic ROS, and that survival
122 requires active detoxification systems.
123
124 **RESULTS**
125 **Starvation-induced antibiotic tolerance in mycobacteria**
126 We first sought to develop conditions suitable for genetic analysis of persister cell survival and
127 stress-induced antibiotic tolerance mycobacteria. Genetic screens examining persister cell
128 physiology face two inherent obstacles. First, these cells are rare in unstressed bacterial
129 populations, and antibiotic-mediated cell death creates population bottlenecks that obscure
130 mutant phenotypes. Second, most mycobacterial populations contain spontaneous drug-resistant

131 mutants that can expand if the population is exposed to a single antibiotic. To overcome these
132 obstacles, we sought to establish large-scale, high-density culture conditions to prevent genetic
133 bottlenecks, and used multiple antibiotics to suppress spontaneous drug-resistant mutants. We
134 began by assessing the feasibility of this approach using wild-type *Msmeg.* We exposed the cells
135 to either the combination of rifampin, isoniazid, and ethambutol (RIF/INH/EMB) used to treat *Mtb*,
136 or to the combination of tigecycline and linezolid (TIG/LZD), two translation-inhibiting antibiotics
137 frequently used to treat *Mabs*[5,37], and empirically determined the minimum inhibitory
138 concentrations (MICs) and minimum bactericidal concentrations (MBC) for each antibiotic under
139 the high-density culture conditions that would be needed for genetic analysis of persister cells.
140 Both antibiotic combinations reduced the bacterial population >1000-fold within 72h (Figure 1A).
141 We then evaluated both spontaneous persister formation and stress-induced tolerance under
142 these conditions in *Msmeg*. We compared logarithmically growing (mid-log) cultures in 7H9 rich
143 media to cultures starved for 2 days in phosphate buffered saline (PBS) prior to addition of
144 antibiotics. Consistent with expectations, we found a marked increase in antibiotic tolerance in
145 starved cultures, with a 100-fold increase in survival following TIG/LZD exposure and a 10,000-
146 fold increase following RIF/INH/EMB exposure (Figure 1A).
147
148 We next examined two species of pathogenic mycobacteria to assess starvation-induced
149 antibiotic tolerance. Both *Mabs* and *Mtb* have been shown to display this response, and we sought
150 to determine whether this could be observed under the conditions needed to conduct a Tn-Seq
151 screen[38-41]. We again compared cells starved in PBS to logarithmically growing cells in 7H9 and
152 found that, under these conditions, cultures of wild-type *Mabs* (ATCC 19977) and *Mtb* (Erdman)
153 displayed dramatic increases antibiotic tolerance in nutrient-deprived cultures (Figure 1B,C).
154 Notably, for *Mabs* and *Msmeg,* the development of tolerance required an adaptation period of
155 several days under starvation conditions, as survival was dramatically impaired if cells were
156 shifted immediately into nutrient-deficient conditions with antibiotics, suggesting that a regulated

157 process needed to be completed. Surprisingly, *Mtb* tolerance developed rapidly without pre-
158 adaptation suggesting that this organism might have additional response pathways enabling more
159 rapid adaptation.
160
161 **Identification of pathways needed for antibiotic tolerance in *Mabs***
162 We used these conditions to carry out Tn-Seq screens in *Mabs* to identify genes necessary for
163 both the survival of spontaneous persister cells and for starvation-induced antibiotic tolerance.
164 We conducted the screen using a *Mabs Himar1* Tn library comprised of ~55,000 mutations across
165 ~91,000 possible TA insertion sites covering all 4,992 non-essential *Mabs* genes in strain ATCC
166 19977[34]. To study spontaneous persister cells, cultures were maintained in continuous log-phase
167 in 7H9 rich media for 48h prior to antibiotic exposure and then exposed to TIG/LZD for 6 days
168 (Figure 2A) a point at which spontaneous persister cells comprise the majority of the population
169 (Figure 1C). To study starvation-induced tolerance, cultures were starved in PBS for 48h prior to
170 antibiotic exposure in PBS. Following antibiotic treatment, cells were then washed and
171 resuspended in antibiotic-free liquid media to recover and passaged 1:100 three times in
172 continuous log-phase to expand surviving cells. We then isolated genomic DNA, sequenced the
173 Tn insertion sites, and used TRANSIT software[42] to quantify the abundance of each Tn mutant
174 across different conditions to identify genes with statistically-significant differences in distribution.
175 We identified 277 *Mabs* genes required for surviving TIG/LZD exposure in rich media, 271 genes
176 required for survival during starvation and 362 genes required to survive the combined exposure
177 to antibiotics and starvation (Log_2 fold-change > 0.5 and Benjamini–Hochberg adjusted p-value
178 (p-adj.) ≤ 0.05; Figure 2B-E). Of the genes required for survival, ~60% were required in both
179 nutrient-replete and starvation states, although condition-specific determinants were also seen
180 (Figure 2F). As expected, we identified genes with already-established functions in antibiotic
181 responses, including *MAB_2752* and *MAB_2753* which are both homologs of known antibiotic
182 transporters in *Mtb,* as well as tetracycline-responsive transcription factors like *MAB_4687* and

183 *MAB_0314c* (Supplemental Table 1), indicating an ability of these Tn-Seq conditions to identify
184 physiologically relevant genes known to mitigate antibiotic stress.
185
186 To identify other cellular processes necessary for survival we performed pathway enrichment
187 analysis on the set of genes identified by Tn-Seq. We used the DAVID[43] analysis tool to perform
188 systematic queries of the KEGG, GO, and Uniprot databases and identify over-represented
189 processes and pathways. Interestingly, although cells were exposed to translation-inhibiting
190 antibiotics, and no exogenous oxidative or nitrosative stress was applied, we identified a number
191 of factors needed to combat these stresses in spontaneous persister cells. This included *bfrB*
192 (bactoferritin), *ahpE* (peroxiredoxin) and *katG* (catalase/peroxidase) as well as 5 components of
193 the bacterial proteasome pathway, known to mediate resistance to nitrosative stress in *Mtb*[44]
194 (Figure 2G, Supplemental Table 2). We also identified multiple members of DNA-damage
195 response pathways including *recF*, *recG*, *uvrA*, *uvrB* and *uvrC*. Examining genes required for
196 starvation-induced tolerance, a number of the same pathways were again seen, and the mutant
197 with the greatest survival defect in this context was *mntH*, a redox-regulated Mn^{2+}/Zn^{2+} transporter
198 implicated in peroxide resistance in other organisms[45, 46].
199
200 To independently confirm a role in antibiotic tolerance for a set of genes from diverse pathways
201 that were identified by Tn-Seq we selected a set of genes required for survival, representing
202 several of the functional pathways identified, and used oligonucleotide-mediated recombineering
203 (ORBIT)[47] to disrupt their open reading frames. The initial genes selected were *pafA* (proteasome
204 pathway), *katG* (catalase-peroxidase), *recR* (DNA repair), *blaR* (β-lactam sensing), and
205 *MAB_1456c* (cobalamin synthesis). To control for non-specific effects of antibiotic selection during
206 the recombineering process, we created a control strain using ORBIT to target a non-coding
207 intergenic region downstream of a redundant tRNA gene (*MAB_t5030c*). We then individually
208 screened each of these mutants to determine if they displayed deficits in survival by exposing

209 cells to TIG/LZD, either in rich 7H9 media or under starvation conditions, as had been done in the
210 Tn-Seq screen. For four out of five mutants we observed defects concordant with the Tn-Seq
211 findings. For Δ*katG* we detected clear defects in survival as soon as 3 days after antibiotic
212 exposure in either rich media or under starvation conditions, corroborating the results of our Tn-
213 Seq analysis (Figure 3A). We observed similar, albeit smaller, defects in the Δ*pafA,* Δ*MAB_1456c*,
214 and Δ*blaR,* mutants under the conditions predicted by the screen (Figure 3B-D). We saw no
215 survival defect in the Δ*recR* mutant (Figure 3E). However, we observed that the Δ*recR* mutant, as
216 well as the Δ*pafA* mutant, instead displayed a marked defect in resumption of growth after removal
217 of antibiotics (Figure 3 – figure supplement 1).
218
219 To further confirm the role of *katG* and *pafA,* and exclude off-target effects of recombineering, we
220 performed genetic complementation analysis by restoring a wild-type copy of each gene into the
221 respective Δ*pafA* and Δ*katG* mutants. In each case, we integrated a single copy of the wild-type
222 gene, under the control of its endogenous promoter, into the genome at the L5 *attB* site (hereafter
223 *pafA+, katG+* strains), and constructed isogenic control strains with an empty vector integrated at
224 the same site (hereafter *pafA-, katG-* strains). We confirmed expression of the re-introduced copy
225 of each gene by RT-qPCR in the *pafA+*, and *katG+* strains, and found expression within roughly
226 2-fold of endogenous wild-type levels (Figure 4A,D). We then challenged these strains with
227 TIG/LZD as before. In rich media, where the Δ*katG* mutants have a moderate survival defect, the
228 *katG+* strain had roughly a 50-fold increase in viable cells relative to the *katG-* strain. We then
229 exposed cells to antibiotics under starvation conditions, where the Δ*katG* mutant phenotype is
230 more severe. Under these conditions the *katG-* cells succumbed rapidly between 3d and 10d after
231 antibiotic exposure, with a 1,000-fold decrease in viable cells relative to control cells, whereas the
232 *katG+* strain showed a near-complete restoration of antibiotic tolerance (Figure 4B). We
233 analogously examined complementation of Δ*pafA* mutants, and although the phenotype of the

234 Δ*pafA* mutant is less severe overall than a Δ*katG* mutant, we saw a similar restoration of survival
235 in *pafA*+ cells relative to *pafA*- cells (Figure 4E). We next evaluated whether the *pafA*-, and *katG*-
236 strains were overall more sensitive to the growth inhibitory effects of TIG/LZD, or whether they
237 had specific defects in survival above the mean bactericidal concentration. We performed MIC
238 determination for TIG and LZD individually for each strain, comparing the *katG*+/*katG*- and
239 *pafA*+/*pafA*- strains. We found that the MICs for each of these strains were unchanged,
240 demonstrating that these mutants were not more readily inhibited by these antibiotics (Figure
241 4C,F). Instead, they have more rapid kinetics of cell death at bactericidal concentrations,
242 consistent with a specific defect in survival, and supporting a model whereby an initial growth-
243 arresting inhibition of the direct antibiotic target can be uncoupled mechanistically from a distinct
244 cell-death step, as has been seen with other antibiotic classes[28].
245
246 **Reactive oxygen contributes to antibiotic lethality in *Mabs***
247 We next investigated the role of KatG and reactive oxygen in antibiotic tolerance more broadly.
248 We began by assessing whether KatG conferred protection from other antibiotics with diverse
249 mechanisms of action, selecting antibiotics that are used clinically for mycobacterial infections.
250 Because *katG*- mutants showed the greatest defects in starvation-induced tolerance, we analyzed
251 survival of *katG*+ and *katG*- strains in starvation-adapted cultures exposed to a panel of different
252 antibiotics. Because both TIG and LZD both act by inhibiting translation, we began by exposing
253 cells to either TIG or LZD alone. As expected, the degree of bacterial killing was significantly less
254 with either agent alone than when they are added in combination. Upon exposure to either of
255 these antibiotics the *katG*- cells died more rapidly than *katG*+ cells, though the final proportion of
256 persister cells in the population was unchanged in *katG*- cells (Figure 5A). When we exposed
257 cells to rifabutin, an RNA polymerase inhibitor, we saw a similar effect, with a 100-fold loss of
258 viability in *katG*- cells relative to the *katG*+ cells (Figure 5B). In contrast, when we exposed
259 cultures to either levofloxacin (topoisomerase inhibitor) or cefoxitin (β-lactam inhibitor of

260 peptidoglycan cross-linking), *katG* had little to no effect on cell viability (Figure 5C-D). Thus, the
261 role of KatG is context-dependent, suggesting that, in *Mabs,* some antibiotics generate oxidative
262 stress that is ameliorated by KatG while others do not.
263
264 The identification of *katG* as essential for cells to survive exposure to TIG/LZD suggests that ROS
265 are present and causing damage. Although TIG and LZD are translation inhibitors that do not
266 directly generate ROS we evaluated whether they might nonetheless be triggering ROS
267 accumulation as a secondary effect. We examined ROS levels in control *Mabs* using the ROS
268 indicator dye cellROX, that is retained in cells when it becomes oxidized[48]. At baseline, during
269 log-phase growth in rich media < 2% of cells had ROS accumulation (Figure 5E). We saw a
270 moderate increase in ROS accumulation in starved cultures, with roughly 7% of the population
271 cellROX+. However, when cells were exposed to antibiotics we saw a dramatic accumulation of
272 ROS, with 57% of cells becoming cellROX+ when exposed to TIG/LZD in rich media and 33% of
273 PBS-starved cells becoming cellROX+ when exposed to TIG/LZD. Taken together, these data
274 indicate that translation inhibition does indeed have important downstream effects on cellular
275 redox balance, with ROS accumulation that could be contributing to the lethal effects of antibiotics.
276
277 We next tested whether ROS were contributing to cell death by reducing ROS production, and
278 then assessing the impact on cell viability. A well-established system for studying hypoxia in
279 mycobacteria is the Wayne Model of gradual-onset hypoxia, whereby low density cultures are
280 inoculated in sealed vessels with minimal headspace. As the culture slowly grows, the soluble
281 oxygen is consumed, resulting in the slow onset of hypoxia over several days, a process that can
282 be monitored by the decolorization of Methylene Blue dye in the media[49]. Under aerobic conditions
283 in rich media, we observed the expected rapid killing of *Mabs* over the first 5 days with the
284 combination of TIG/LZD, with more rapid loss of viability in KatG- cells. However, under hypoxic
285 conditions, where ROS production is suppressed, we saw much slower bacterial killing.

286 Importantly, under hypoxic conditions *katG*- cells no longer had a survival defect relative to *katG*+
287 cells, supporting the hypothesis that translation-inhibiting antibiotics also cause secondary
288 accumulation of lethal ROS in antibiotic-treated cells that need to be detoxified by KatG (Figure
289 5F).
290
291 We also evaluated whether other methods of alleviating ROS damage might enhance survival.
292 The iron chelator 2,2'-dipyridyl has been shown in other contexts to reduce ROS-mediated
293 damage by suppressing the reaction of H_20_2 with Fe^{2+} that generates highly oxidizing hydroxyl
294 radicals (Fenton reaction), and which has been shown to mitigate oxidative damage in other
295 bacteria following antibiotic exposure[25, 28, 50]. As seen in other bacteria, we find that in *Mabs*, 2,2'-
296 dipyridy does indeed improve bacterial survival following exposure to bactericidal translation
297 inhibitors, further supporting a role in ROS in cell death following translation inhibition (Figure 5G).
298
299 We also assessed whether free radical scavengers like thiourea and 2,2,6,6-
300 tetramethylpiperidine-1-oxyl (TEMPO) ameliorated antibiotic toxicity, although similar thiol
301 antioxidants had previously been shown in *Mtb* to increase respiration and ROS generation and
302 to paradoxically decrease bacterial survival upon INH exposure[30]. When we treated *Mabs*
303 simultaneously with TIG/LZD in combination with either thiourea or TEMPO we did not observe a
304 restoration of antibiotic tolerance, and, similar to observations in *Mtb,* actually observed increased
305 bacterial cell death (Figure 5 – figure supplement 1).
306
307 **Antibiotic-induced ROS accumulation is conserved but reliance on KatG is variable among**
308 ***Mabs* strains**
309 To test whether ROS accumulation was an effect occurring more broadly across different *Mabs*
310 strains we obtained two clinical strains, exposed them to TIG/LZD in 7H9 media, and measured
311 ROS accumulation with cellROX as above. We found that similar to ATCC 19977, both clinical

312 *Mabs* strains had elevated ROS levels following translation inhibition (Figure 6A), suggesting that
313 this is a conserved process in *Mabs*. Next, we tested the role of KatG in these *Mabs* clinical
314 strains. We used ORBIT to disrupt the *katG* locus and evaluated the ability of these Δ*katG* clinical
315 strains to survive exposure to TIG/LZD under both stressed and un-stressed conditions. Unlike
316 ROS accumulation, where the responses across strains were consistent, we saw a variable
317 dependency on *katG*. Clinical strain-1 behaved differently overall, with no appreciable starvation-
318 induced antibiotic tolerance, and no contribution of *katG* to survival. In contrast, for clinical strain-
319 2, *katG* contributed significantly to starvation-induced antibiotic tolerance, behaving similarly to
320 the ATCC 19977 reference strain. However, unlike the reference strain, *katG* was not required for
321 survival of clinical strain-2 when exposed to antibiotics in 7H9 media (Figure 6B). Thus, although
322 antibiotic-induced ROS accumulation was observed across all three *Mabs* strains, the Δ*katG*
323 phenotype displays incomplete penetrance, suggesting that in some *Mabs* strains alternative
324 pathways exist that are able to compensate for the loss of *katG.*
325
326 **DISCUSSION:**
327 The results of these studies point to an important effect of ROS in amplifying the lethality of
328 transcription and translation-inhibiting antibiotics in *Mabs*. Through genetic analysis we identified
329 a number of ROS detoxification factors, including KatG, as necessary for survival in this context.
330 This suggested that antibiotics induced an oxidative state in cells, and direct measurement of
331 ROS following antibiotic exposure indicated that this was indeed the case. Further supporting the
332 toxic effects of ROS in this context, we found that removal of oxygen both slowed bacterial killing
333 and rendered KatG dispensable. Taken together, these results suggest that in *Mabs* antibiotic
334 lethality is accelerated by ROS accumulation, and that survival requires active detoxification
335 systems.
336

337 **Pathways necessary for antibiotic tolerance in *Mabs.***

338 The phenomenon of antibiotic tolerance has been recognized for decades and has been observed
339 in a broad array of bacterial species[10, 51-57] but without identification of a singular underlying
340 mechanism conserved among species - suggesting that different pathways may play roles in
341 different physiologic contexts. For example, the pathways identified in one bacterial species may
342 not contribute to tolerance in another. In *E. coli, relA* plays an important role in stress-induced
343 tolerance, as it does in *Pseudomonas aeruginosa*[52], *Staphylococcus aureus*[53], and *Mtb*[54].
344 However, its role is not universal. Deletion of *relA* had no effect on antibiotic tolerance in *Msmeg*[55],
345 and in our Tn-Seq analysis, *Mabs relA* Tn mutants had no survival defect. In the case of *Mabs*
346 this may be due to genetic redundancy, as a prior study of the *Mabs relA* mutant demonstrated
347 that this strain still synthesizes (p)ppGpp[58]. In addition, even within a single species there can be
348 differences in the critical survival mechanisms depending on the context. In *E. coli,* RelA
349 contributes strongly to persister viability following exposure to β-lactams, but not
350 aminoglycosides[56], and in our study we find KatG to be essential for tolerance to transcription and
351 translation inhibitors but not to a β-lactam (cefoxitin) or a quinolone (levofloxacin).

352

353 **Mechanisms of antibiotic lethality**

354 Our findings strongly support the idea that antibiotic-induced ROS can be a significant contributor to
355 bactericidal activity in *Mabs* and contribute to the growing evidence that this phenomenon is conserved
356 across diverse types of bacteria. In mycobacteria, other groups have observed that hypoxia
357 reduced antibiotic-mediated killing in *Mabs, Mtb* and *Msmeg*, and in *Mtb*, exposure to rifampin or
358 moxifloxacin also generates ROS, with *katG* contributing to survival in rifampin-treated cells[28, 29].
359 Notably, we found evidence for ROS mediated bactericidal activity with the translation inhibiting
360 antibiotics tigecycline and linezolid, as well as the transcription inhibiting antibiotic rifabutin. This
361 contrasts with findings in *E. coli* where the rifamycins and tetracyclines are not bactericidal and

362 do not induce ROS[25, 26], suggesting that mycobacteria-specific responses may exist that result in
363 lethal ROS production.
364
365 Exactly how transcription or translation blockade leads to increased ROS levels is not known. In
366 principle, any of several derangements could lead to ROS accumulation. One of the major
367 sources of cellular ROS is oxidative phosphorylation, as hydrogen peroxide and superoxide are
368 natural byproducts. Thus, increased ROS generation by oxidative phosphorylation is an attractive
369 hypothesis. Alternatively, particularly under starvation conditions, it is possible that antioxidants
370 and ROS scavengers may become depleted, creating a more oxidizing environment. Our Tn-Seq
371 analysis provides additional insight on this. We noted a small class of Tn mutants that were
372 paradoxically protected from antibiotic lethality (Figure 2B). Prominent among this class of
373 mutants were several independent components of the NADH dehydrogenase complex. Also
374 known as Complex I of the electron transport chain, it is one of the key entry points for electrons
375 into the oxidative phosphorylation pathway. The observation that mutants lacking this complex
376 are protected suggests that decreasing flux through oxidative phosphorylation, with a concomitant
377 decrease in ROS generation, may enhance survival during antibiotic exposure. A mechanistic
378 understanding of how blockade of either transcription or translation leads to deranged oxygen
379 utilization is an unresolved question that will require further study.
380
381 ROS accumulation is not universal following exposure to bactericidal antibiotics. While antibiotic-
382 induced ROS is well-documented, under some conditions, such as higher concentrations of
383 antibiotic, multiple studies have also observed antibiotic lethality without ROS accumulation[59-62].
384 Similarly, prior studies have found that under certain conditions, *E. coli* mutants lacking catalase
385 have defects in antibiotic tolerance[63-65], whereas under other conditions they do not[59] . In *Mabs*
386 the role of *katG* was also not uniform, as it had no impact on survival following exposure to
387 levofloxacin or cefoxitin. Additional studies will be needed to determine whether levofloxacin and

388 cefoxitin kill without generating ROS, or whether ROS is generated but effectively detoxified by
389 other systems in the absence of *katG.* This latter possibility is suggested by our findings in *Mabs*
390 clinical strains. While we saw ROS accumulation in all strains after TIG/LZD exposure, the role of
391 *katG* was variable between the strains. This suggests that compensatory pathways likely exist
392 and that in *Mabs* they can overcome the loss of *katG.*
393
394 **Therapeutic implications**
395 *Mabs* infections are particularly challenging to treat, and frequently have poor outcomes[4]. Our
396 results highlight several bacterial processes, such as the bacterial proteasome and ROS
397 detoxification, which might be targeted therapeutically to reduce the survival of antibiotic tolerant
398 bacteria in patients with *Mabs* infection. Agents targeting these processes might not have any
399 intrinsic antimicrobial activity alone, but might act to disrupt the unique physiology required to
400 survive antibiotics. This would represent a new therapeutic class of "persistence inhibitors" that
401 might act synergistically with traditional antibiotics to eliminate the subpopulation of cells that
402 would otherwise remain viable, despite prolonged antibiotic treatment, in patients with *Mabs* and
403 other chronic infections[28, 30].
404
405 **Limitations**
406 Tn-Seq has inherent drawbacks, including an inability to identify mutants in essential genes, or in
407 cases of genetic redundancy. Thus, there are likely genes needed for antibiotic tolerance in *Mabs*
408 that were not identified in this study. In addition, we studied the response to a single class of
409 antibiotic, focusing on the translation inhibitors often used to treat *Mabs* infections, and we studied
410 only spontaneous persister cells and starvation-induced antibiotic tolerance. It is likely that
411 examining other antibiotics, with different mechanisms of action, or different stresses that induce
412 tolerance would identify additional genes contributing to survival and would allow identification of
413 core pathways that might be shared in differing physiologic contexts of antibiotic and stress.

414

415 **MATERIALS AND METHODS**

416 **Key Reagent Table**

Reagent	Source/Reference	Identifier
***Mabs* ATCC 19977**	ATCC	19977
***Msmeg* MC2 155**	ATCC	700084
***Mtb* Erdman**	ATCC	35801
***Mabs* clinical strains**	Sacramento Department of Public Health	--
pkm444	Addgene	108319
pkm496	Addgene	109301
pmv306	Ref.66	--
Middlebrook 7H9	BD	271310
Middlebrook 7H10	BD	262710
Glycerol	Invitrogen	15514011
Tween-80	Fisher	BP338-500
Middlebrook OADC	BD	212351
DPBS (-Ca/Mg)	Gibco	14190144
Tyloxapol	Sigma Aldrich	T8761
Methylene blue	Sigma Aldrich	28514
Tigecycline	Chem Impex	29737
Linezolid	Chem Impex	29723
Levofloxacin	Sigma Aldrich	28266
Cefoxitin	Chem Impex	1490
Rifabutin	Cayman Chemical	16468

Rifampin	Sigma Aldrich	R7382
Isoniazid	Supelco	I3377
Ethambutol	Thermo Scientific	J6069506
DMSO	Sigma Aldrich	D2650
Trizol	Invitrogen	15596018
0.1mm zirconia beads	Biospec	11079101z
PureLink RNA Mini Kit	Invitrogen	12183025
Kanamycin	VWR	75856-686
Zeocin	Invivogen	ANTZN1P
Glycine	Fisher Bioreagents	BP381
Sucrose	Sigma Aldrich	S1888
Anhydrotetracycline	Cayman Chemical	10009542
cellROX green	Invitrogen	C10444
Paraformaldehyde	Sigma Aldrich	P6148
DAPI	Sigma Aldrich	D9542
DNAseI	New England Biolabs	M0303
Maxima H minus reverse transcriptase	Thermo Scientific	EP0752
Taq Polymerase	New England Biolabs	M0273
EvaGreen	Biotium	31019
2,2′-Bipyridyl - 2,2′-Bipyridine	Sigma Aldrich	D216305
Thiourea	Sigma Aldrich	T7875
4-Hydroxy-TEMPO	Sigma Aldrich	176141

417

418 Bacterial strains and culture conditions:

419 *Mabs* ATCC 19977, clinical *Mabs* strains and *Msmeg* (MC2 155) were grown in BD Middlebrook
420 7H9 media (liquid) or 7H10 media (solid) supplemented with 0.5% glycerol (Sigma) and 0.2%
421 Tween-80 (Fisher) but without any OADC supplementation except for transformations.
422 Sacramento clinical isolates were obtained from the Sacramento County Department of Public
423 Health Mycobacteriology Laboratory. Confirmation of clinical isolates as *Mabs* was performed by
424 amplifying the 16s rRNA locus and Sanger sequencing (Supplemental Table 4). *Mtb* (Erdman)
425 was grown in 7H9 (liquid) or 7H10 (solid) supplemented with 0.5% glycerol, 0.1% Tween-80, and
426 10% OADC (BD). All cultures were grown at 37°C with gentle shaking. Except for specific hypoxia
427 conditions, all liquid cultures were grown with 90% container headspace or using a gas permeable
428 cap to ensure culture oxygenation. PBS starvation was achieved by washing OD 0.5-1.0 *Mabs*
429 1X in DPBS (-Ca/Mg, Gibco) and resuspending in DPBS at OD=1, supplemented with 0.1%
430 tyloxapol (Sigma).
431
432 *Mabs* antibiotic experiments:
433 For PBS starvation experiments, stocks of *Mabs* were grown for 48 hours in 7H9 passaging
434 continuously in log phase, then either PBS starved or passaged in log phase for an additional 48
435 h. Log phase or PBS starved *Mabs* were then resuspended in antibiotic containing media at
436 OD1.0. For experiments with hypoxia, *Mabs* in mid-log aerobic growth was adjusted to OD 0.001
437 in media with 1.5 μg/ml methylene blue and added to a rubber septum sealed glass vial with 50%
438 headspace. Methylene blue discoloration was observed at 3d and antibiotics were added at 5d.
439 For thiourea and TEMPO experiments, these were added to the cultures at the time of antibiotic
440 administration. For bipyridyl experiments, 62.5 μM bipyridyl was added to the cultures 2h prior to
441 antibiotic administration. We empirically determined the half-life of each antibiotic in 7H9 media
442 at 37-deg and for those with half-lives shorter than the experiment, supplemented cultures to with
443 additional antibiotic to maintain the concentration of active antibiotic. Antibiotics were used at the
444 following concentrations: tigecycline (Chem-Impex) at 10 μg/ml (8-fold above MIC, re-

445 administered every 3 days), linezolid (Chem-Impex) at 100 µg/ml (20-fold above MIC),
446 levofloxacin (Sigma) at 40µg/ml (8-fold above MIC), cefoxitin (Chem Impex) at 80 µg/ml (8-fold
447 above MIC, re-administered every 3 days), and rifabutin (Cayman) at 40µg/ml (4-fold above MIC).
448 After antibiotic administration, colony forming units over time were measured by plating on 7H10
449 solid media. For experiments where growth recovery time in liquid media was quantified, 100µl of
450 sample was removed at d6 after antibiotic administration and washed 2X in antibiotic-free media.
451 The samples were resuspended in 5ml of antibiotic free media, and OD620 measurements were
452 taken with a FilterMax F3 plate reader (Molecular Devices) until maximum cell density (OD of
453 ~5.0) was reached.
454
455 *Msmeg* antibiotic experiments:
456 Individual colonies were picked and grown for 48 hours in log phase before being PBS starved or
457 passaged in log phase for 48h. Log phase or PBS starved *Msmeg* were then resuspended in
458 antibiotic containing media at OD1.0. Antibiotics were used at the following concentrations:
459 tigecycline (Chem-Impex) at 1.25 µg/ml (8-fold above MIC, re-administered every 3 days),
460 linezolid (Chem-Impex) at 2.5 µg/ml (8 fold above MIC), rifampin (Sigma) at 32 µg/ml (8-fold above
461 MIC, re-administered every 6 days), isoniazid (Sigma) at 32 µg/ml (8-fold above MIC, re-
462 administered every 6 days), and ethambutol (Thermo) at 4 µg/ml (8-fold above MIC, re-
463 administered every 3 days). After antibiotic administration, colony forming units over time were
464 measured.
465
466 *Mtb* antibiotic experiments:
467 Freezer stocks of *Mtb* were thawed and grown for 5-7 days in log phase before being starved for
468 14d or longer. Non-starved control *Mtb* were thawed such that they were also grown for 5-7 days
469 in log phase before experimental use. Log phase or PBS starved *Mtb* was then resuspended in
470 antibiotic containing media and adjusted to OD 1.0. Antibiotics were used at the following

471 concentrations: rifampin (Sigma) at 0.1 μg/ml (4-fold above MIC, re-administered every 6 days),
472 isoniazid (Sigma) at 0.1μg/ml (4-fold above MIC, re-administered every 6 days), and ethambutol
473 (Thermo) at 8 μg/ml (4-fold above MIC, re-administered every 6 days). After antibiotic
474 administration, colony forming units over time were measured.
475
476 Transposon insertion sequencing:
477 The construction of this *Himar1* transposon Tn library has been described previously[34]. Screening
478 was performed by growing a freezer stock of the library for 2.5 days in log phase before 48 h PBS
479 starvation or further continuous log-phase growth. Samples were then resuspended in media
480 containing either tigecycline/linezolid or an equal volume of DMSO solvent and incubated for 6
481 days, with a re-administration of tigecycline or matching DMSO on day 3. Cultures were aerated
482 by culturing in a vented cap bottle with gentle agitation at 40 revolutions per minute throughout
483 the experiment. The samples were then washed 2X in antibiotic free liquid media, resuspended
484 in antibiotic free liquid media (10X the original culture volume), and grown until OD=0.5-1.0.
485 Subsequently, the samples underwent three more rounds of 100-fold passaging in liquid media
486 to amplify surviving bacteria before the samples were collected in Trizol (Invitrogen). A sample
487 taken at the time of the commencement of PBS starvation was collected in Trizol and used as the
488 input control. Three independent trials of this experiment were submitted to the UC Davis DNA
489 Technologies Core, where Tn insertion site flanking sequences were amplified as described
490 previously[34] and sequenced on an Element Biosciences AVITI. Sequence reads were mapped to
491 the ATCC 19977 genome and analyzed using TRANSIT software with the following parameters:
492 0% of N/C termini ignored, 10,000 samples, TTR normalization, LOESS correction, include sites
493 with all zeros, site restricted resampling. Genes with significant changes were defined as those
494 with adjusted p-value (p-adj.) <0.05 and $\log_2$ fold change >0.5. P-adj. was calculated using the
495 Benjamini-Hochberg correction.
496

497 Pathway enrichment analysis

498 To improve gene annotation, *Mabs* orthologs to *Mtb* genes were identified. *Mabs* genes were first
499 converted into protein sequences using Mycobrowser, and protein sequences were then used to
500 perform reciprocal BLASTp searches. *Mabs* genes and *Mtb* genes that mapped to each other
501 using independent one-way BLASTp searches with a maximum e-value cutoff of 0.1 were
502 considered orthologs. For pathway analysis, gene lists (*Mtb* orthologs) were then imported into
503 the DAVID knowledgebase[43] and pathway enrichment analysis performed for Gene Ontology
504 biological process, Uniprot keyword and KEGG databases with statistical analysis Fisher's exact
505 test and nominal p-value reported.

506

507 Gene deletion and complementation:

508 Knockout strains were generated using ORBIT[47]. Briefly, *Mabs* was transformed with the
509 kanamycin-resistant ORBIT recombineering plasmid pkm444. 20ml *Mabs* at OD=0.5-1.0 was
510 washed 2X in 10% glycerol and resuspended in 200ul 10% glycerol. 500ng plasmid was added
511 and electroporated at 2.5kV in 0.2cm cuvettes. The bacteria were allowed to recover overnight
512 before plating on 150µg/ml kanamycin plates. Clones were selected and regrown in liquid media
513 supplemented with 150µg/ml kanamycin and 10% OADC (BD) to OD0.5-1.0. For recombineering,
514 the pkm444-*Mabs* was grown to mid-log, then diluted to OD0.1 and 200mM glycine (Fisher) was
515 added to the media. 16 h later, 500mM sucrose (Sigma) and 500 ng/ml anhydrotetracycline
516 (Cayman) were added and incubated for an additional 4 h. Subsequently, the *Mabs* was washed
517 2X in ice cold 10% glycerol + 500mM sucrose. 200ul of 10X concentrated *Mabs* was then
518 electroporated with 600ng of the zeocin-R ORBIT payload pkm496 plasmid and 2µg of targeting
519 oligonucleotide (Table S3) at 2.5kV in 0.2cm cuvettes. The *Mabs* was then allowed to recover
520 overnight in liquid media with 10% OADC and 500ng/ml anhydrotetracycline before being plated
521 on 150 µg/ml zeocin plates. Mutants were then selected and screened for gene deletion by PCR
522 amplification and Sanger sequencing. For genetic complementation, the endogenous loci

523 including promoter and terminator sequences were amplified by PCR and cloned into the EcoRV
524 site of pmv306 with kanamycin resistance[66]. In the case of *katG,* the upstream gene *furA* was
525 also included in the complementation construct to achieve optimal *katG* expression.
526
527 MIC determination
528 Two-fold serial dilutions of antibiotics were prepared in a 96 well plate in 100ul volume. 100ul of
529 2X bacteria were added (for *Mabs*: used a final OD of 0.001, *Msmeg*: OD0.001, *Mtb*: OD0.01),
530 making a final volume of 200µl. The plates were incubated until there was visible growth in the no
531 antibiotic control well. At this time, the bacteria were transferred to a new plate with 20µl of 40%
532 paraformaldehyde and OD620 measurements were taken with a FilterMax F3 plate reader
533 (Molecular Devices). MIC values for wild-type ATCC 19977 under these conditions are listed in
534 Supplemental Table 5.
535
536 Flow cytometry
537 A culture of OD=1.0 *Mabs* was stained with cellROX green (Invitrogen) at a final concentration
538 of 5µM for 1hr at 37C. The cells were then washed in PBS and resuspended in PBS with 4%
539 paraformaldehyde and 5 µg/ml DAPI (Sigma). The samples were run on an LSRII flow cytometer
540 (BD). Fluorophores were excited with the 405nm (DAPI) and 488nm (cellROX) lasers. Detection
541 was performed using the 450/50 (505LP) filter for DAPI and a 525/50 (555LP) filter for cellROX.
542 Data were analyzed with FlowJo software (BD).
543
544 DNA/RNA Purification:
545 Samples were resuspended in 5 volumes of Trizol, and bead beat with 0.1mm zirconia beads
546 (Biospec) 6x2min at 4°C in a Mini-Beadbeater-16 (Biospec). Chloroform was added and RNA in
547 the aqueous phase removed. For DNA isolation, a second RNA extraction was performed with
548 0.8M guanidine thiocyanate and 0.5M guanidine hydrochloride, 60mM Acetate pH 5.2, 1mM

549 EDTA. DNA was then isolated with back-extraction buffer (4M Guanidine Thiocyanate, 50mM
550 Sodium Citrate, 1M Tris base (without pH adjustment ~pH 11) and DNA purified using a PureLink
551 RNA Mini Kit (Invitrogen).
552
553 RT-qPCR
554 RNA was purified using PureLink RNA Mini Kit per manufacturer's instructions. The samples were
555 DNAseI (NEB) treated for 15min/37°C before stopping the reaction by adding 3.5mM EDTA and
556 heating for 10min/75°C. cDNA was synthesized from 500ng total RNA using random hexamers
557 and Maxima H minus reverse transcriptase (Thermo). No reverse-transcription controls were also
558 included and used to confirm the lack of genomic DNA-driven amplification. qPCR reactions used
559 Taq polymerase (NEB) and EvaGreen (Biotium) and were run on Biorad CFX Opus 96 Real-Time
560 PCR System. Melt curves were included for each sample to confirm uniform amplicon identity
561 between samples. Gene-specific amplification was quantified by comparison to a standard curve
562 generated from 3-fold serial dilutions of a control sample, then normalized to 16S rRNA within
563 each sample.
564
565 **FIGURE LEGENDS**
566 **Figure 1. Starvation induces antibiotic tolerance in diverse mycobacteria.** (A) *Msmeg,* (B)
567 *Mtb* or (C) *Mabs* were grown in 7H9 rich media or starved in PBS prior to the addition of antibiotics
568 and surviving colony forming units (CFU) enumerated. For the rapidly growing mycobacteria,
569 *Msmeg* and *Mabs,* cells were allowed to adapt for 48h prior to antibiotics, for slow-growing *Mtb,*
570 cells were allowed to adapt for 14-21d prior to antibiotics. Samples without pre-adaptation were
571 washed and placed directly into PBS with antibiotics. Antibiotic concentrations were: *Msmeg* -
572 Isoniazid (INH) 32μg/ml (8 x MIC), rifampin (RIF) 32 μg/ml (8 x MIC), ethambutol (EMB) 4μg/ml
573 (8 x MIC), tigecycline (TIG) 1.25 μg/ml (8 x MIC), linezolid (LZD) 2.5 μg/ml (8 x MIC). *Mtb* – RIF
574 0.1 μg/ml (4 x MIC), INH at 0.1 μg/ml (4 x MIC), EMB at 8 μg/ml (4 x MIC). *Mabs* – TIG 10 μg/ml

575 (8 x MIC), LZD 100 μg/ml (20 x MIC). Antibiotics with half-lives shorter than the duration of
576 experiment were re-added at the following intervals: TIG, EMB every 3d; RIF, INH every 6d. Error
577 bars represent SEM, statistical significance is calculated at each time point using student's t test.
578 ****: $p<0.0001$, ***: $p<0.001$, **: $p<0.01$, *: $p<0.05$, ns: $p>0.05$. Data are combined from 3
579 independent experiments.
580
581 **Figure 2. Tn-Seq identifies genes required for antibiotic tolerance in *Mabs*.** (A) Experimental
582 design. (B-E) Tn-Seq analysis showing relative abundance of individual genes under the indicted
583 conditions. For (B-D) gene abundance in each condition is measured relative the input with
584 negative values for genes depleted in each experimental condition relative to the input. Log_2 fold-
585 change is on x-axis with $-log_{10}$ of the p-value on y-axis. All cultures were fully aerated throughout
586 the experiment and cultures without antibiotics received and equal volume of DMSO. In (E) an
587 additional comparison is made for PBS with antibiotics relative to the PBS condition. Genes with
588 significant decreases in abundance are shown in color (p-adj. < 0.05 and log_2 fold-change > 0.5)
589 using the Benjamini–Hochberg adjustment for multiple hypothesis testing. (F) Number of genes
590 essential in each condition relative to the input population. (G) Pathway enrichment analysis of
591 the essential genes in each condition using the DAVID knowledgebase ($p <0.05$). Screens were
592 run as 3 independent experiments and the combined results analyzed. Antibiotic conditions were
593 as described above.
594
595 **Figure 3. Validation of Tn-Seq results.** (A-E) ORBIT homologous recombination was used to
596 delete the indicated genes, or to generate a control strain targeting a distant intergenic region
597 distal to the non-essential tRNA gene *MAB_t5030c*. Each strain was either grown in 7H9 rich
598 media or starved in PBS for 48 prior to the addition of antibiotics as indicated. The conditions
599 tested here correspond to the conditions in the Tn-Seq analysis where a phenotype was observed.
600 Comparisons in panels A-C are made to the same control strain but plotted independently for

601 clarity. Error bars represent SEM, statistical significance is calculated at each time point using
602 student's t test. ****: p<0.0001, ***: p<0.001, **: p<0.01, *: p<0.05, ns: p>0.05. Antibiotics were
603 added as described above. Data are representative of 4 independent experiments.
604 Figure supplement 1. Additional analysis of mutants
605
606 **Figure 4. Complementation analysis of *katG* and *pafA* mutants confirms their role in**
607 **antibiotic tolerance.** (A) RT-qPCR analysis of *katG* expression in *katG- (Δ katG::pmv306), katG+*
608 *(Δ katG::pmv306 katG),* and control strain (ORBIT intergenic*::pmv306*). (B) CFU over time for
609 *katG+/katG-* strains. (C) MICs for *katG+/katG-* strains. (D) Expression of *pafA in pafA-*
610 *(Δ pafA::pmv306), pafA+* (*pafA::pmv306 pafA*) and control strain. (E) CFU over time for
611 *pafA+/pafA-* strains. (F) MICs for *pafA+/pafA-* strains. Antibiotic concentrations in (A-B, D-E) are
612 as described above. Error bars represent SEM, statistical significance is calculated at each time
613 point using student's t test between *katG+/katG-* strains in (B) and between *pafA+/pafA-* strains
614 in (E). ****: p<0.0001, ***: p<0.001, **: p<0.01, *: p<0.05, ns: p>0.05. Antibiotics were added as
615 described above.
616
617 **Figure 5. ROS-mediated toxicity following antibiotic exposure.** (A-D) Analysis of
618 *katG+/katG-* cells challenged with different antibiotics. Cells were starved in PBS for 48h and
619 then exposed to the indicated antibiotic. (E) Flow cytometry of control cells exposed to TIG/LZD
620 (4h in 7H9 media or 72h in PBS) and then stained with DAPI and the ROS-sensitive dye
621 cellROX green; percentage cellROX-positive cells are indicated. (F) Survival over time for
622 aerated and hypoxic cultures of *Mabs* after exposure to TIG/LZD. (G) Survival over time for
623 bipyridyl treated cells after exposure to TIG/LZD. Error bars represent SEM, statistical
624 significance is calculated at each time point using student's t test. ****: p<0.0001, ***: p<0.001,

625 **: p<0.01, *: p<0.05, ns: p>0.05. (A-D, F) display combined data from 3 independent
626 experiments. (E, G) are representative data from 3 independent experiments.
627 Figure supplement 1. Effect of ROS scavengers.
628
629 **Figure 6. Conserved antibiotic-induced ROS production but variable protection by KatG**
630 **among different *Mabs* strains.** (A) The indicated strains of *Mabs* were cultured in 7H9 media,
631 exposed to TIG/LZD for 4h and then analyzed by cellROX staining. (B) CFU over time following
632 TIG/LZD exposure. Error bars represent SEM, statistical significance is calculated at each time
633 point using student's t test. ****: p<0.0001, ***: p<0.001, **: p<0.01, *: p<0.05, ns: p>0.05.
634 Combined data from 4 independent experiments are shown for persister survival experiments.
635 Representative data from 2 independent experiments are shown for flow cytometry experiments.
636 Antibiotics were added as described above.
637
638 **Figure 3 – figure supplement 1. Additional analysis of mutants.** (A) *blaR* or (B) *recR* mutants
639 were examined under conditions where Tn-Seq did not predict a phenotype. Cells were starved
640 in PBS for 48h prior to treatment with TIG/LZD or DMSO as described in Figure 3. (C) Growth
641 recovery of mutants after antibiotic exposure. After 6 d of TIG/LZD exposure cells were washed
642 twice in antibiotic free media and inoculated into 7H9 media. Growth was monitored by OD 600
643 of the culture. Error bars represent SEM, statistical significance is calculated at each time point
644 using student's t test. ****: p<0.0001, ***: p<0.001, **: p<0.01, *: p<0.05, ns: p>0.05. (A-B) are
645 representative data from 4 independent experiments (C) is representative data from 2
646 independent experiments.
647
648 **Figure 5 – figure supplement 1. Effect of ROS scavengers.** *ΔkatG* cells were starved in PBS
649 for 48h then treated with TIG/LZD and the indicated concentration of (A) thiourea or (B) TEMPO

650 and surviving CFU over time were measured. Representative data from 2 independent
651 experiments are shown.
652
653 **Supplemental Table 1. Tn-Seq results**
654 **Supplemental Table 2. DAVID functional pathway analysis**
655 **Supplemental Table 3. Oligonucleotide sequences**
656 **Supplemental Table 4. 16s sequencing data of clinical strains**
657 **Supplemental Table 5. MIC Values**
658
659 **ACKNOWLEDGEMENTS**
660 We would like to thank Nick Campbell-Kruger for his technical insights on identifying *Mabs/Mtb*
661 orthologs, Jonathan Van Dyke for his assistance with flow cytometry analysis, Emily Kumimoto
662 and Siranoosh Ashtari for their assistance with Tn-Seq library preparation and sequencing, and
663 Jessie Li and Bradley Jenner for their assistance with Tn-seq bioinformatics. We would also like
664 to thank Caroline Dominic at the Sacramento County Department of Public Health for providing
665 clinical isolates of *Mabs* for analysis.
666
667 **FUNDING**
668 Pew Biomedical Scholars Fellowship BHP
669 NIH R01 1R01AI144149 BHP
670 NIH R01 1R01AI143722 SAS
671 NIH T32 HL007013 AR
672 NIH Shared Instrumentation Grant 1S10OD010786-01 DNA Technologies and Expression
673 Analysis Core, UC Davis Genome Center
674 NCI Cancer Center Support Grant P30CA093373 Flow Cytometry Shared Resource, UC Davis
675

676 **CONFLICTS OF INTEREST**

677 BHP and SAS serve on the scientific advisory board of X-Biotics Therapeutics.

678

679

680 **REFERENCES**

681

682

683 1. Stevens, D.L., A.L. Bisno, H.F. Chambers, E.P. Dellinger, E.J. Goldstein, S.L. Gorbach,
684 J.V. Hirschmann, S.L. Kaplan, J.G. Montoya, and J.C. Wade, *Practice guidelines for the*
685 *diagnosis and management of skin and soft tissue infections: 2014 update by the*
686 *Infectious Diseases Society of America.* Clin Infect Dis, 2014. **59**(2): p. e10-52.
687 2. Metersky, M.L. and A.C. Kalil, *Management of ventilator-associated pneumonia:*
688 *guidelines.* Clinics in chest medicine, 2018. **39**(4): p. 797-808.
689 3. Nahid, P., S.E. Dorman, N. Alipanah, P.M. Barry, J.L. Brozek, A. Cattamanchi, L.H.
690 Chaisson, R.E. Chaisson, C.L. Daley, and M. Grzemska, *Official American thoracic*
691 *society/centers for disease control and prevention/infectious diseases society of America*
692 *clinical practice guidelines: treatment of drug-susceptible tuberculosis.* Clinical infectious
693 diseases, 2016. **63**(7): p. e147-e195.
694 4. Griffith, D.E. and C.L. Daley, *Treatment of Mycobacterium abscessus Pulmonary*
695 *Disease.* CHEST, 2022. **161**(1): p. 64-75.
696 5. Griffith, D.E., T. Aksamit, B.A. Brown-Elliott, A. Catanzaro, C. Daley, F. Gordin, S.M.
697 Holland, R. Horsburgh, G. Huitt, and M.F. Iademarco, *An official ATS/IDSA statement:*
698 *diagnosis, treatment, and prevention of nontuberculous mycobacterial diseases.*
699 American journal of respiratory and critical care medicine, 2007. **175**(4): p. 367-416.

700 6. Meylan, S., I.W. Andrews, and J.J. Collins, *Targeting Antibiotic Tolerance, Pathogen by*
701 *Pathogen.* Cell, 2018. **172**(6): p. 1228-1238.
702 7. Namugenyi, S.B., A.M. Aagesen, S.R. Elliott, and A.D. Tischler, *Mycobacterium*
703 *tuberculosis PhoY Proteins Promote Persister Formation by Mediating Pst/SenX3-*
704 *RegX3 Phosphate Sensing.* mBio, 2017. **8**(4): p. e00494-17.
705 8. Liu, Y., S. Tan, L. Huang, R.B. Abramovitch, K.H. Rohde, M.D. Zimmerman, C. Chen, V.
706 Dartois, B.C. VanderVen, and D.G. Russell, *Immune activation of the host cell induces*
707 *drug tolerance in Mycobacterium tuberculosis both in vitro and in vivo.* Journal of
708 Experimental Medicine, 2016. **213**(5): p. 809-825.
709 9. Gold, B. and C. Nathan, *Targeting Phenotypically Tolerant Mycobacterium tuberculosis.*
710 Microbiol Spectr, 2017. **5**(1).
711 10. Bigger, J., *Treatment of Staphyloeoeeal Infections with Penicillin by Intermittent*
712 *Sterilisation.* Lancet, 1944: p. 497-500.
713 11. Ronneau, S., P.W.S. Hill, and S. Helaine, *Antibiotic persistence and tolerance: not just*
714 *one and the same.* Current opinion in microbiology, 2021. **64**: p. 76-81.
715 12. Dhar, N. and J.D. McKinney, *Microbial phenotypic heterogeneity and antibiotic tolerance.*
716 Current opinion in microbiology, 2007. **10**(1): p. 30-38.
717 13. Grant, S.S., B.B. Kaufmann, N.S. Chand, N. Haseley, and D.T. Hung, *Eradication of*
718 *bacterial persisters with antibiotic-generated hydroxyl radicals.* Proceedings of the
719 National Academy of Sciences, 2012. **109**(30): p. 12147-12152.
720 14. Baker, J.J. and R.B. Abramovitch, *Genetic and metabolic regulation of Mycobacterium*
721 *tuberculosis acid growth arrest.* Scientific Reports, 2018. **8**(1).
722 15. Saito, K., T. Warrier, S. Somersan-Karakaya, L. Kaminski, J. Mi, X. Jiang, S. Park, K.
723 Shigyo, B. Gold, and J. Roberts, *Rifamycin action on RNA polymerase in antibiotic-*
724 *tolerant Mycobacterium tuberculosis results in differentially detectable populations.*
725 Proceedings of the National Academy of Sciences, 2017. **114**(24): p. E4832-E4840.

726 16. Hipolito, V.E.B., E. Ospina-Escobar, and R.J. Botelho, *Lysosome remodelling and*
727 *adaptation during phagocyte activation.* Cell Microbiol, 2018. **20**(4).
728 17. Sukumar, N., S. Tan, B.B. Aldridge, and D.G. Russell, *Exploitation of Mycobacterium*
729 *tuberculosis reporter strains to probe the impact of vaccination at sites of infection.* PLoS
730 Pathog, 2014. **10**(9): p. e1004394.
731 18. Schumacher, M.A., K.M. Piro, W. Xu, S. Hansen, K. Lewis, and R.G. Brennan, *Molecular*
732 *Mechanisms of HipA-Mediated Multidrug Tolerance and Its Neutralization by HipB.*
733 Science, 2009. **323**(5912): p. 396-401.
734 19. Kusser, W. and E.E. Ishiguro, *Suppression of mutations conferring penicillin tolerance by*
735 *interference with the stringent control mechanism of Escherichia coli.* Journal of
736 Bacteriology, 1987. **169**(9): p. 4396-4398.
737 20. Rodionov, D.G. and E.E. Ishiguro, *Direct correlation between overproduction of*
738 *guanosine 3',5'-bispyrophosphate (ppGpp) and penicillin tolerance in Escherichia coli.*
739 Journal of Bacteriology, 1995. **177**(15): p. 4224-4229.
740 21. Bokinsky, G., E.E.K. Baidoo, S. Akella, H. Burd, D. Weaver, J. Alonso-Gutierrez, H.
741 García-Martín, T.S. Lee, and J.D. Keasling, *HipA-Triggered Growth Arrest and β-Lactam*
742 *Tolerance in Escherichia coli Are Mediated by RelA-Dependent ppGpp Synthesis.*
743 Journal of Bacteriology, 2013. **195**(14): p. 3173-3182.
744 22. Korch, S.B., T.A. Henderson, and T.M. Hill, *Characterization of the hipA7 allele of*
745 *Escherichia coli and evidence that high persistence is governed by (p)ppGpp synthesis.*
746 Mol Microbiol, 2003. **50**(4): p. 1199-213.
747 23. Harms, A., C. Fino, A. Sørensen Michael, S. Semsey, and K. Gerdes, *Prophages and*
748 *Growth Dynamics Confound Experimental Results with Antibiotic-Tolerant Persister*
749 *Cells.* mBio, 2017. **8**(6): p. 10.1128/mbio.01964-17.

750 24. Wong, F., S. Wilson, R. Helbig, S. Hegde, O. Aftenieva, H. Zheng, C. Liu, T. Pilizota, E.C.
751 Garner, A. Amir, and L.D. Renner, *Understanding Beta-Lactam-Induced Lysis at the*
752 *Single-Cell Level.* Frontiers in Microbiology, 2021. **12**.
753 25. Kohanski, M.A., D.J. Dwyer, B. Hayete, C.A. Lawrence, and J.J. Collins, *A common*
754 *mechanism of cellular death induced by bactericidal antibiotics.* Cell, 2007. **130**(5): p.
755 797-810.
756 26. Dwyer, D.J., P.A. Belenky, J.H. Yang, I.C. MacDonald, J.D. Martell, N. Takahashi, C.T.Y.
757 Chan, M.A. Lobritz, D. Braff, E.G. Schwarz, J.D. Ye, M. Pati, M. Vercruysse, P.S. Ralifo,
758 K.R. Allison, A.S. Khalil, A.Y. Ting, G.C. Walker, and J.J. Collins, *Antibiotics induce*
759 *redox-related physiological alterations as part of their lethality.* Proceedings of the
760 National Academy of Sciences, 2014. **111**(20): p. E2100-E2109.
761 27. Zeng, J., Y. Hong, N. Zhao, Q. Liu, W. Zhu, L. Xiao, W. Wang, M. Chen, S. Hong, L. Wu,
762 Y. Xue, D. Wang, J. Niu, K. Drlica, and X. Zhao, *A broadly applicable, stress-mediated*
763 *bacterial death pathway regulated by the phosphotransferase system (PTS) and the*
764 *cAMP-Crp cascade.* Proc Natl Acad Sci U S A, 2022. **119**(23): p. e2118566119.
765 28. Shee, S., S. Singh, A. Tripathi, C. Thakur, T.A. Kumar, M. Das, V. Yadav, S. Kohli, R.S.
766 Rajmani, N. Chandra, H. Chakrapani, K. Drlica, and A. Singh, *Moxifloxacin-Mediated*
767 *Killing of Mycobacterium tuberculosis Involves Respiratory Downshift, Reductive Stress,*
768 *and Accumulation of Reactive Oxygen Species.* Antimicrob Agents Chemother, 2022.
769 **66**(9): p. e0059222.
770 29. Saito, K., S. Mishra, T. Warrier, N. Cicchetti, J. Mi, E. Weber, X. Jiang, J. Roberts, A.
771 Gouzy, E. Kaplan, C.D. Brown, B. Gold, and C. Nathan, *Oxidative damage and delayed*
772 *replication allow viable Mycobacterium tuberculosis to go undetected.* Sci Transl Med,
773 2021. **13**(621): p. eabg2612.
774 30. Vilchèze, C., T. Hartman, B. Weinrick, P. Jain, T.R. Weisbrod, L.W. Leung, J.S.
775 Freundlich, and W.R. Jacobs, Jr., *Enhanced respiration prevents drug tolerance and*

776 *drug resistance in Mycobacterium tuberculosis.* Proc Natl Acad Sci U S A, 2017. **114**(17):
777 p. 4495-4500.
778 31. Augusto Cesar, H.-S., J.P. Brian, B. Joseph, and C.B. Cara, *Mycobacterium abscessus*
779 *Cells Have Altered Antibiotic Tolerance and Surface Glycolipids in Artificial Cystic*
780 *Fibrosis Sputum Medium.* Antimicrobial Agents and Chemotherapy, 2019. **63**(7): p.
781 e02488-18.
782 32. Li, S., N.C. Poulton, J.S. Chang, Z.A. Azadian, M.A. DeJesus, N. Ruecker, M.D.
783 Zimmerman, K.A. Eckartt, B. Bosch, and C.A. Engelhart, *CRISPRi chemical genetics*
784 *and comparative genomics identify genes mediating drug potency in Mycobacterium*
785 *tuberculosis.* Nature microbiology, 2022. **7**(6): p. 766-779.
786 33. Carey, A.F., J.M. Rock, I.V. Krieger, M.R. Chase, M. Fernandez-Suarez, S. Gagneux,
787 J.C. Sacchettini, T.R. Ioerger, and S.M. Fortune, *TnSeq of Mycobacterium tuberculosis*
788 *clinical isolates reveals strain-specific antibiotic liabilities.* PLoS pathogens, 2018. **14**(3):
789 p. e1006939.
790 34. Rodriguez, R., N. Campbell-Kruger, J. Gonzalez Camba, J. Berude, R. Fetterman, and
791 S. Stanley, *MarR-Dependent Transcriptional Regulation of mmpSL5 Induces*
792 *Ethionamide Resistance in Mycobacterium abscessus.* Antimicrobial Agents and
793 Chemotherapy, 2023. **67**(4): p. e01350-22.
794 35. Kreutzfeldt, K.M., R.S. Jansen, T.E. Hartman, A. Gouzy, R. Wang, I.V. Krieger, M.D.
795 Zimmerman, M. Gengenbacher, J.P. Sarathy, M. Xie, V. Dartois, J.C. Sacchettini, K.Y.
796 Rhee, D. Schnappinger, and S. Ehrt, *CinA mediates multidrug tolerance in*
797 *Mycobacterium tuberculosis.* Nat Commun, 2022. **13**(1): p. 2203.
798 36. Bellerose, M.M., S.-H. Baek, C.-C. Huang, C.E. Moss, E.-I. Koh, M.K. Proulx, C.M.
799 Smith, R.E. Baker, J.S. Lee, S. Eum, S.J. Shin, S.-N. Cho, M. Murray, and C.M. Sassetti,
800 *Common Variants in the Glycerol Kinase Gene Reduce Tuberculosis Drug Efficacy.*
801 mBio, 2019. **10**(4): p. e00663-19.

802 37. Kumar, K., C.L. Daley, D.E. Griffith, and M.R. Loebinger, *Management of Mycobacterium*
803 *avium complex and Mycobacterium abscessus pulmonary disease: therapeutic*
804 *advances and emerging treatments.* European respiratory review, 2022. **31**(163).
805 38. Yam, Y.-K., N. Alvarez, M.-L. Go, and T. Dick, *Extreme Drug Tolerance of Mycobacterium*
806 *abscessus "Persisters".* Frontiers in Microbiology, 2020. **11**.
807 39. Berube, B.J., L. Castro, D. Russell, Y. Ovechkina, and T. Parish, *Novel Screen to Assess*
808 *Bactericidal Activity of Compounds Against Non-replicating Mycobacterium abscessus.*
809 Front Microbiol, 2018. **9**: p. 2417.
810 40. Lee, J., N. Ammerman, A. Agarwal, M. Naji, S.Y. Li, and E. Nuermberger, *Differential In*
811 *Vitro Activities of Individual Drugs and Bedaquiline-Rifabutin Combinations against*
812 *Actively Multiplying and Nutrient-Starved Mycobacterium abscessus.* Antimicrob Agents
813 Chemother, 2021. **65**(2).
814 41. Betts, J.C., P.T. Lukey, L.C. Robb, R.A. McAdam, and K. Duncan, *Evaluation of a*
815 *nutrient starvation model of Mycobacterium tuberculosis persistence by gene and protein*
816 *expression profiling.* Molecular microbiology, 2002. **43**(3): p. 717-731.
817 42. DeJesus, M.A., C. Ambadipudi, R. Baker, C. Sassetti, and T.R. Ioerger, *TRANSIT-a*
818 *software tool for Himar1 TnSeq analysis.* PLoS computational biology, 2015. **11**(10): p.
819 e1004401.
820 43. Huang da, W., B.T. Sherman, and R.A. Lempicki, *Systematic and integrative analysis of*
821 *large gene lists using DAVID bioinformatics resources.* Nat Protoc, 2009. **4**(1): p. 44-57.
822 44. Darwin, K.H., S. Ehrt, J.-C. Gutierrez-Ramos, N. Weich, and C.F. Nathan, *The*
823 *proteasome of Mycobacterium tuberculosis is required for resistance to nitric oxide.*
824 Science, 2003. **302**(5652): p. 1963-1966.
825 45. Shi, H., R. Zhang, L. Lan, Z. Chen, and J. Kan, *Zinc mediates resuscitation of lactic acid-*
826 *injured Escherichia coli by relieving oxidative stress.* Journal of Applied Microbiology,
827 2019. **127**(6): p. 1741-1750.

828 46. Hohle, T.H. and M.R. O'Brian, *The mntH gene encodes the major Mn(2+) transporter in*
829 *Bradyrhizobium japonicum and is regulated by manganese via the Fur protein.* Mol
830 Microbiol, 2009. **72**(2): p. 399-409.
831 47. Murphy, K.C., S.J. Nelson, S. Nambi, K. Papavinasasundaram, C.E. Baer, and C.M.
832 Sassetti, *ORBIT: a new paradigm for genetic engineering of mycobacterial*
833 *chromosomes.* mBio, 2018. **9**(6): p. e01467-18.
834 48. McBee, M.E., Y.H. Chionh, M.L. Sharaf, P. Ho, M.W.L. Cai, and P.C. Dedon, *Production*
835 *of superoxide in bacteria is stress- and cell state-dependent: A gating-optimized flow*
836 *cytometry method that minimizes ROS measurement artifacts with fluorescent dyes.*
837 Frontiers in Microbiology, 2017. **8**(MAR).
838 49. Wayne, L.G. and L.G. Hayes, *An In Vitro Model for Sequential Study of Shiftdown of*
839 *Mycobacterium tuberculosis through Two Stages of Nonreplicating Persistence.* Infection
840 and Immunity, 1996. **64**(6): p. 2062-2069.
841 50. Winterbourn, C.C., *Toxicity of iron and hydrogen peroxide: the Fenton reaction.* Toxicol
842 Lett, 1995. **82-83**: p. 969-74.
843 51. Moyed, H.S. and K.P. Bertrand, *hipA, a newly recognized gene of Escherichia coli K-12*
844 *that affects frequency of persistence after inhibition of murein synthesis.* Journal of
845 Bacteriology, 1983. **155**(2): p. 768-775.
846 52. Viducic, D., T. Ono, K. Murakami, H. Susilowati, S. Kayama, K. Hirota, and Y. Miyake,
847 *Functional analysis of spoT, relA and dksA genes on quinolone tolerance in*
848 *Pseudomonas aeruginosa under nongrowing condition.* Microbiol Immunol, 2006. **50**(4):
849 p. 349-57.
850 53. Geiger, T., B. Kästle, F.L. Gratani, C. Goerke, and C. Wolz, *Two small (p)ppGpp*
851 *synthases in Staphylococcus aureus mediate tolerance against cell envelope stress*
852 *conditions.* J Bacteriol, 2014. **196**(4): p. 894-902.

853 54. Dutta, N.K., L.G. Klinkenberg, M.J. Vazquez, D. Segura-Carro, G. Colmenarejo, F.
854 Ramon, B. Rodriguez-Miquel, L. Mata-Cantero, E. Porras-De Francisco, Y.M. Chuang,
855 H. Rubin, J.J. Lee, H. Eoh, J.S. Bader, E. Perez-Herran, A. Mendoza-Losana, and P.C.
856 Karakousis, *Inhibiting the stringent response blocks Mycobacterium tuberculosis entry*
857 *into quiescence and reduces persistence.* Sci Adv, 2019. **5**(3): p. eaav2104.
858 55. Bhaskar, A., C. De Piano, E. Gelman, J.D. McKinney, and N. Dhar, *Elucidating the role*
859 *of (p) ppGpp in mycobacterial persistence against antibiotics.* IUBMB life, 2018. **70**(9): p.
860 836-844.
861 56. Wu, N., L. He, P. Cui, W. Wang, Y. Yuan, S. Liu, T. Xu, S. Zhang, J. Wu, W. Zhang, and
862 Y. Zhang, *Ranking of persister genes in the same Escherichia coli genetic background*
863 *demonstrates varying importance of individual persister genes in tolerance to different*
864 *antibiotics.* Front Microbiol, 2015. **6**: p. 1003.
865 57. Zeng, J., Y. Hong, N. Zhao, Q. Liu, W. Zhu, L. Xiao, W. Wang, M. Chen, S. Hong, L. Wu,
866 Y. Xue, D. Wang, J. Niu, K. Drlica, and X. Zhao, *A broadly applicable, stress-mediated*
867 *bacterial death pathway regulated by the phosphotransferase system (PTS) and the*
868 *cAMP-Crp cascade.* Proceedings of the National Academy of Sciences, 2022. **119**(23):
869 p. e2118566119.
870 58. Hunt-Serracín, A.C., M.I. Kazi, J.M. Boll, and C.C. Boutte, *In Mycobacterium abscessus,*
871 *the Stringent Factor Rel Regulates Metabolism but Is Not the Only (p)ppGpp Synthase.*
872 J Bacteriol, 2022. **204**(2): p. e0043421.
873 59. Liu, Y. and J.A. Imlay, *Cell death from antibiotics without the involvement of reactive*
874 *oxygen species.* Science, 2013. **339**(6124): p. 1210-3.
875 60. Keren, I., Y. Wu, J. Inocencio, L.R. Mulcahy, and K. Lewis, *Killing by bactericidal*
876 *antibiotics does not depend on reactive oxygen species.* Science, 2013. **339**(6124): p.
877 1213-6.

878 61. Mahoney, T.F. and T.J. Silhavy, *The Cpx stress response confers resistance to some, but*
879 *not all, bactericidal antibiotics.* J Bacteriol, 2013. **195**(9): p. 1869-74.
880 62. Ezraty, B., A. Vergnes, M. Banzhaf, Y. Duverger, A. Huguenot, A.R. Brochado, S.Y. Su, L.
881 Espinosa, L. Loiseau, B. Py, A. Typas, and F. Barras, *Fe-S cluster biosynthesis controls*
882 *uptake of aminoglycosides in a ROS-less death pathway.* Science, 2013. **340**(6140): p.
883 1583-7.
884 63. Goswami, M., S.H. Mangoli, and N. Jawali, *Involvement of Reactive Oxygen Species in*
885 *the Action of Ciprofloxacin against Escherichia coli.* Antimicrobial Agents and
886 Chemotherapy, 2006. **50**(3): p. 949-954.
887 64. Wang, X. and X. Zhao, *Contribution of oxidative damage to antimicrobial lethality.*
888 Antimicrob Agents Chemother, 2009. **53**(4): p. 1395-402.
889 65. Hong, Y., Q. Li, Q. Gao, J. Xie, H. Huang, K. Drlica, and X. Zhao, *Reactive oxygen*
890 *species play a dominant role in all pathways of rapid quinolone-mediated killing.* J
891 Antimicrob Chemother, 2020. **75**(3): p. 576-585.
892 66. Snapper, S.B., L. Lugosi, A. Jekkel, R.E. Melton, T. Kieser, B.R. Bloom, and W.R.
893 Jacobs, Jr., *Lysogeny and transformation in mycobacteria: stable expression of foreign*
894 *genes.* Proc Natl Acad Sci U S A, 1988. **85**(18): p. 6987-91.

895

FIGURE 1

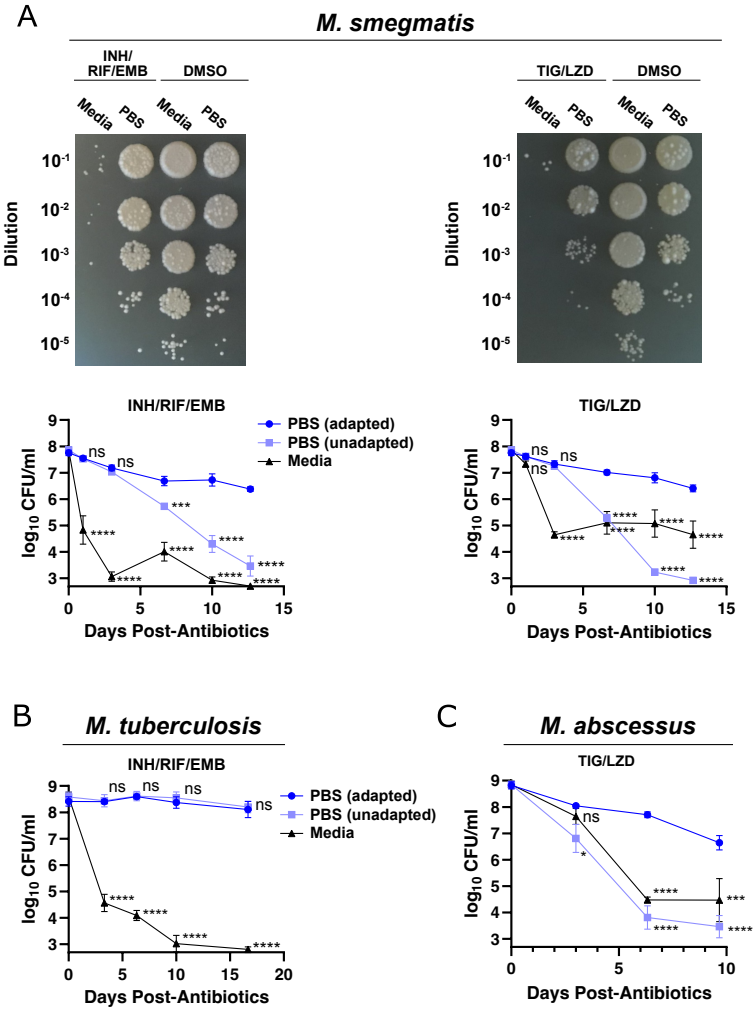
A
M. smegmatis
INH/ RIF/EMB
DMSO
TIG/LZD
DMSO
Media
PBS
Media
PBS
Dilution
10-1
10-2
10-3
10-4
10-5
INH/RIF/EMB
TIG/LZD
PBS (adapted)
PBS (unadapted)
Media
log10 CFU/ml
Days Post-Antibiotics
ns
***
****

B
M. tuberculosis
INH/RIF/EMB
PBS (adapted)
PBS (unadapted)
Media
log10 CFU/ml
Days Post-Antibiotics
ns
****

C
M. abscessus
TIG/LZD
log10 CFU/ml
Days Post-Antibiotics
ns
*
***
****

FIGURE 2

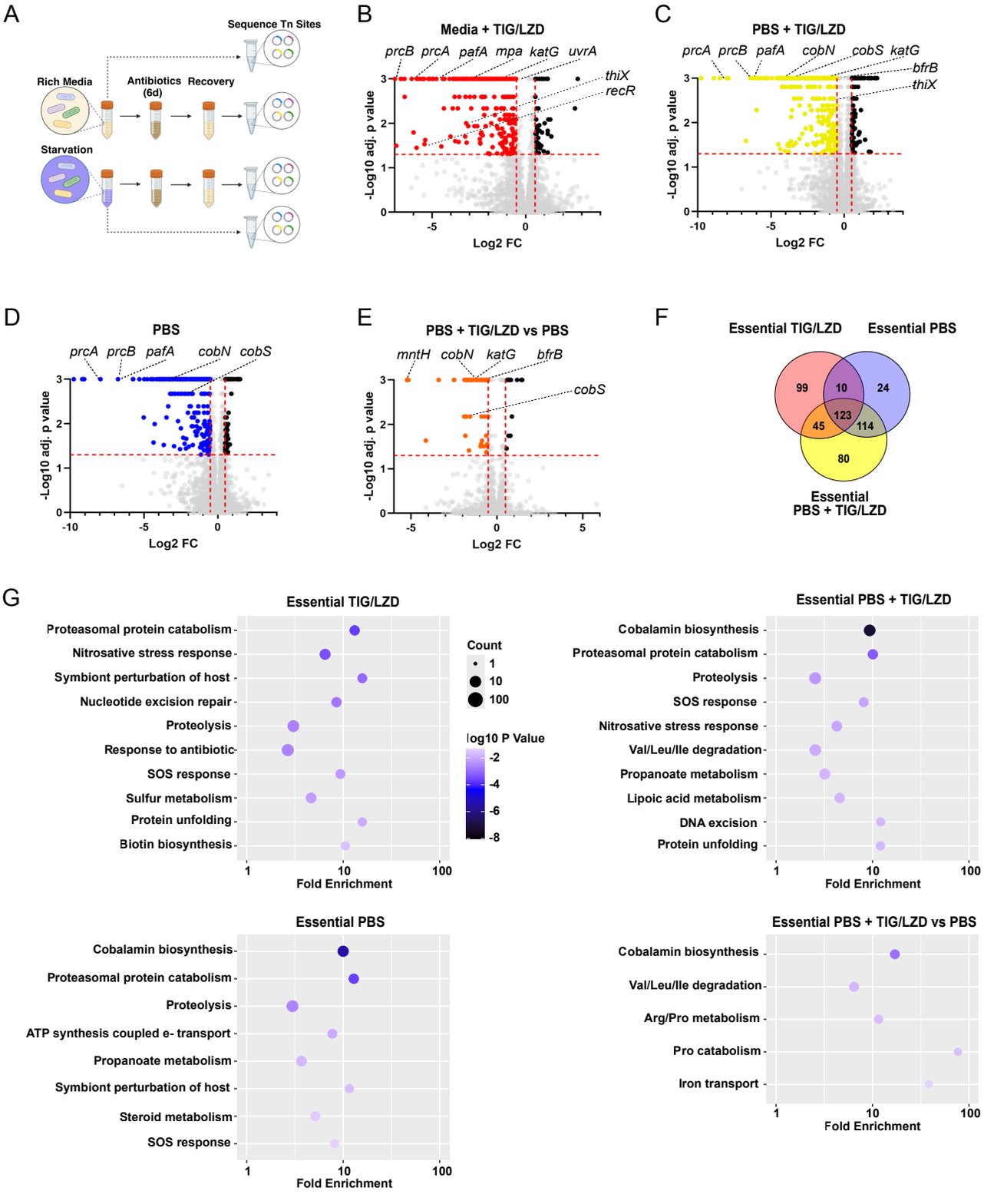
A
Sequence Tn Sites
Rich Media
Antibiotics (6d)
Recovery
Starvation
B
Media + TIG/LZD
prcB prcA pafA mpa katG uvrA
thiX
recR
-Log10 adj. p value
Log2 FC
C
PBS + TIG/LZD
prcA prcB pafA cobN cobS katG
bfrB
thiX
-Log10 adj. p value
Log2 FC
D
PBS
prcA prcB pafA cobN cobS
-Log10 adj. p value
Log2 FC
E
PBS + TIG/LZD vs PBS
mntH cobN katG bfrB
cobS
-Log10 adj. p value
Log2 FC
F
Essential TIG/LZD
Essential PBS
99
10
24
123
45
114
80
Essential PBS + TIG/LZD
G
Essential TIG/LZD
Proteasomal protein catabolism
Nitrosative stress response
Symbiont perturbation of host
Nucleotide excision repair
Proteolysis
Response to antibiotic
SOS response
Sulfur metabolism
Protein unfolding
Biotin biosynthesis
Fold Enrichment
Count
1
10
100
log10 P Value
-2
-4
-6
-8
Essential PBS + TIG/LZD
Cobalamin biosynthesis
Proteasomal protein catabolism
Proteolysis
SOS response
Nitrosative stress response
Val/Leu/Ile degradation
Propanoate metabolism
Lipoic acid metabolism
DNA excision
Protein unfolding
Fold Enrichment
Essential PBS
Cobalamin biosynthesis
Proteasomal protein catabolism
Proteolysis
ATP synthesis coupled e- transport
Propanoate metabolism
Symbiont perturbation of host
Steroid metabolism
SOS response
Fold Enrichment
Essential PBS + TIG/LZD vs PBS
Cobalamin biosynthesis
Val/Leu/Ile degradation
Arg/Pro metabolism
Pro catabolism
Iron transport
Fold Enrichment

FIGURE 3

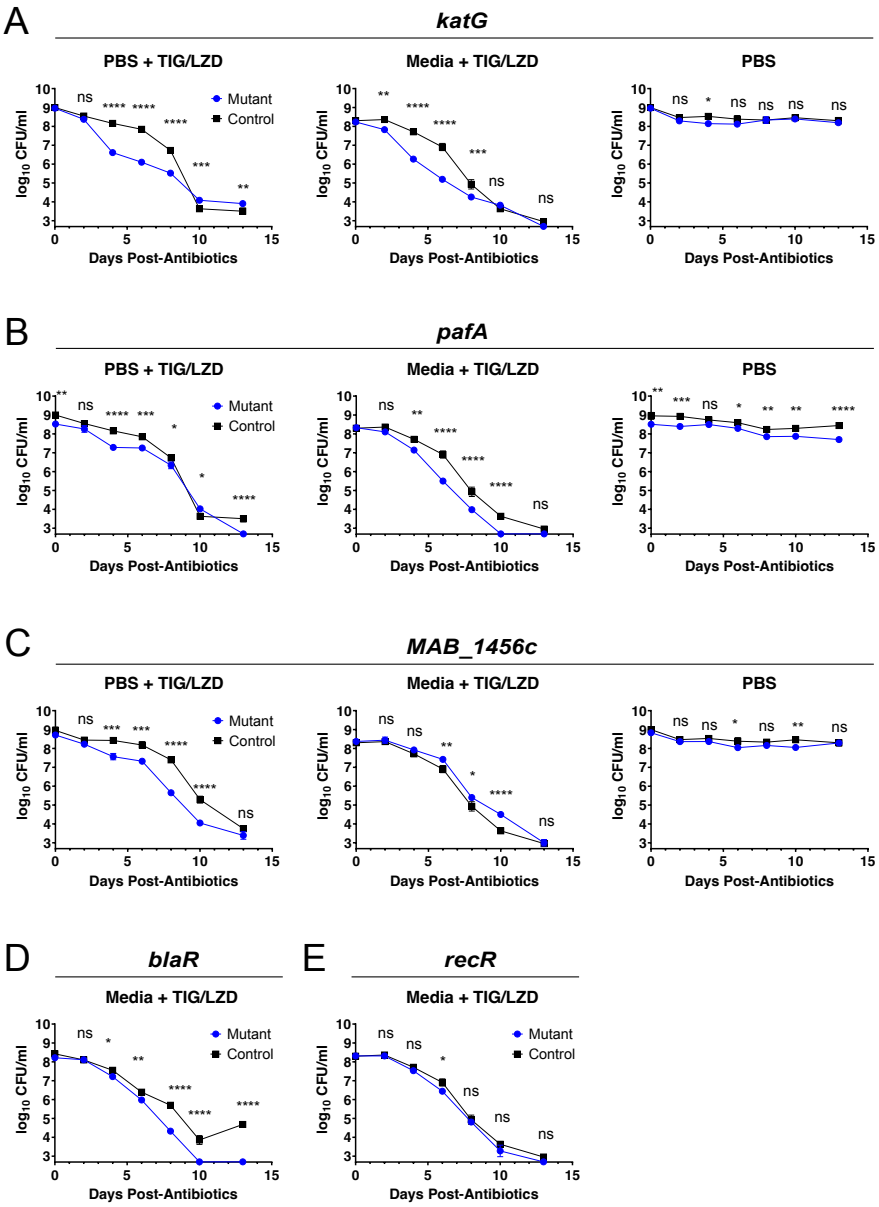
A
katG
PBS + TIG/LZD
Media + TIG/LZD
PBS
Mutant
Control
log10 CFU/ml
Days Post-Antibiotics
B
pafA
C
MAB_1456c
D
blaR
E
recR

FIGURE 4

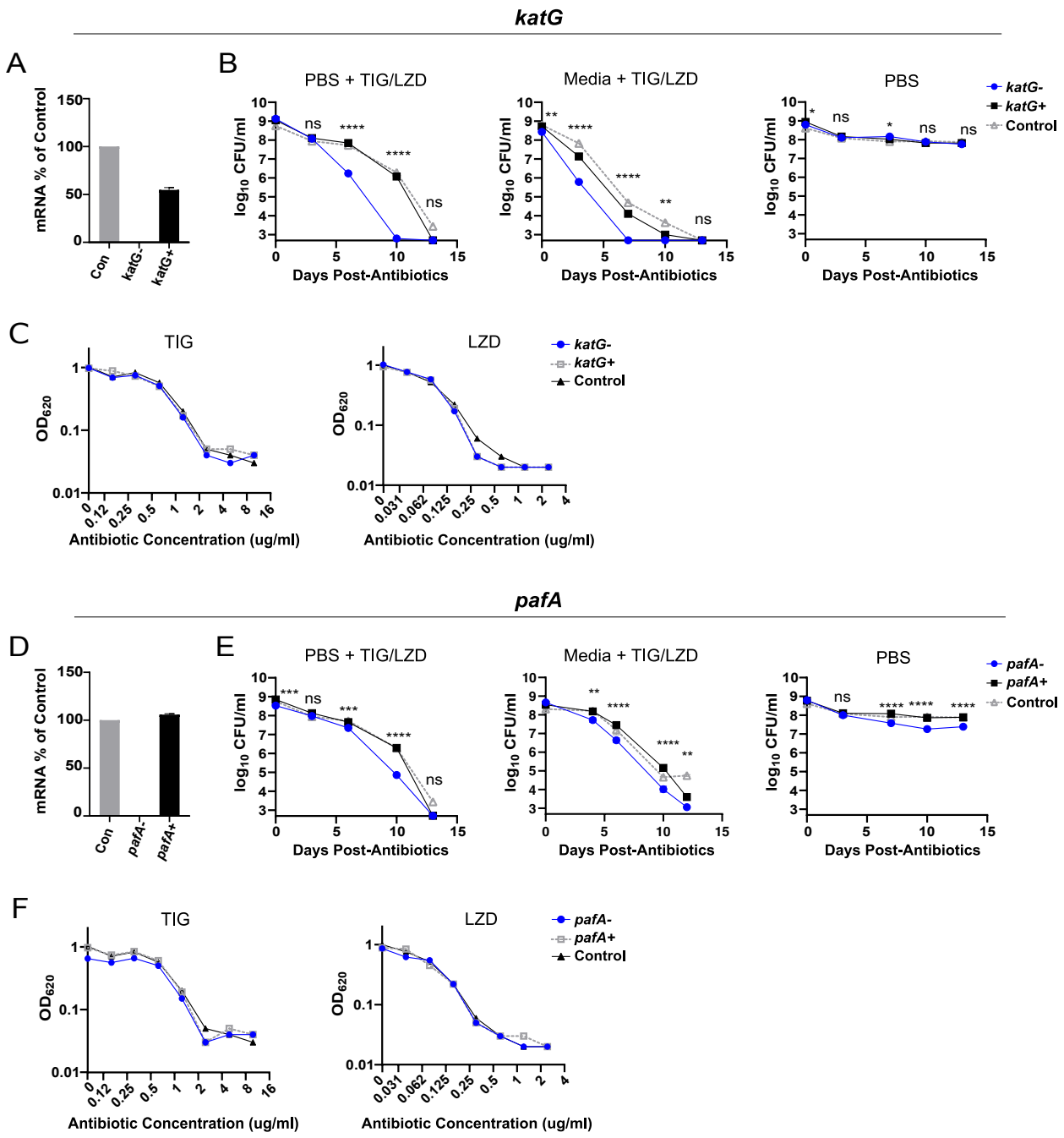
katG
A
mRNA % of Control
Con
katG-
katG+
B
PBS + TIG/LZD
Media + TIG/LZD
PBS
log10 CFU/ml
Days Post-Antibiotics
katG-
katG+
Control
C
TIG
LZD
OD620
Antibiotic Concentration (ug/ml)
pafA
D
mRNA % of Control
Con
pafA-
pafA+
E
PBS + TIG/LZD
Media + TIG/LZD
PBS
log10 CFU/ml
Days Post-Antibiotics
pafA-
pafA+
Control
F
TIG
LZD
OD620
Antibiotic Concentration (ug/ml)

FIGURE 5

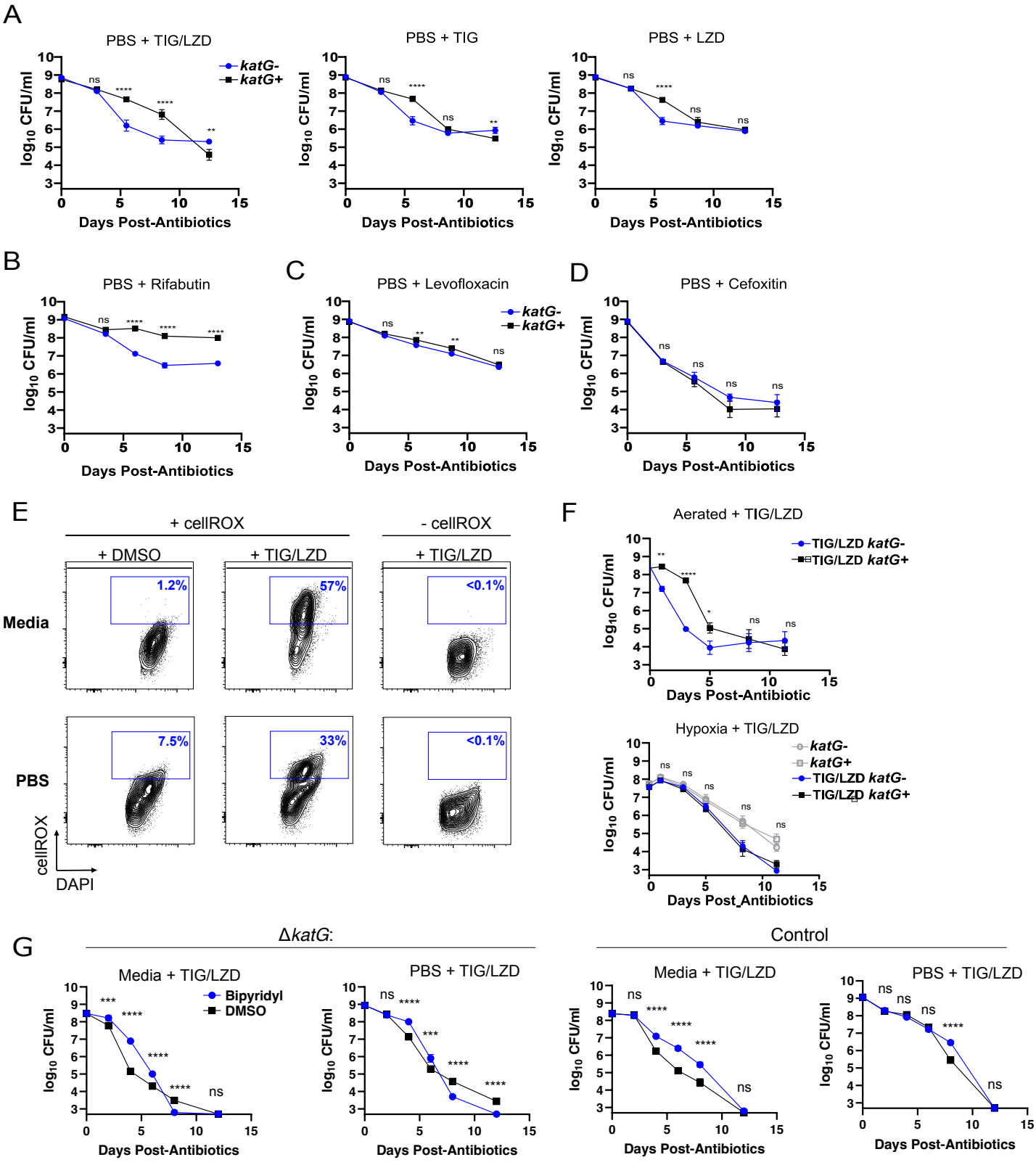
A
PBS + TIG/LZD
PBS + TIG
PBS + LZD
katG-
katG+
log10 CFU/ml
Days Post-Antibiotics
B
PBS + Rifabutin
C
PBS + Levofloxacin
D
PBS + Cefoxitin
E
+ cellROX
- cellROX
+ DMSO
+ TIG/LZD
Media
PBS
1.2%
57%
<0.1%
7.5%
33%
<0.1%
cellROX
DAPI
F
Aerated + TIG/LZD
TIG/LZD katG-
TIG/LZD katG+
Days Post-Antibiotic
Hypoxia + TIG/LZD
Days Post_Antibiotics
G
ΔkatG:
Control
Media + TIG/LZD
PBS + TIG/LZD
Bipyridyl
DMSO

FIGURE 6

A

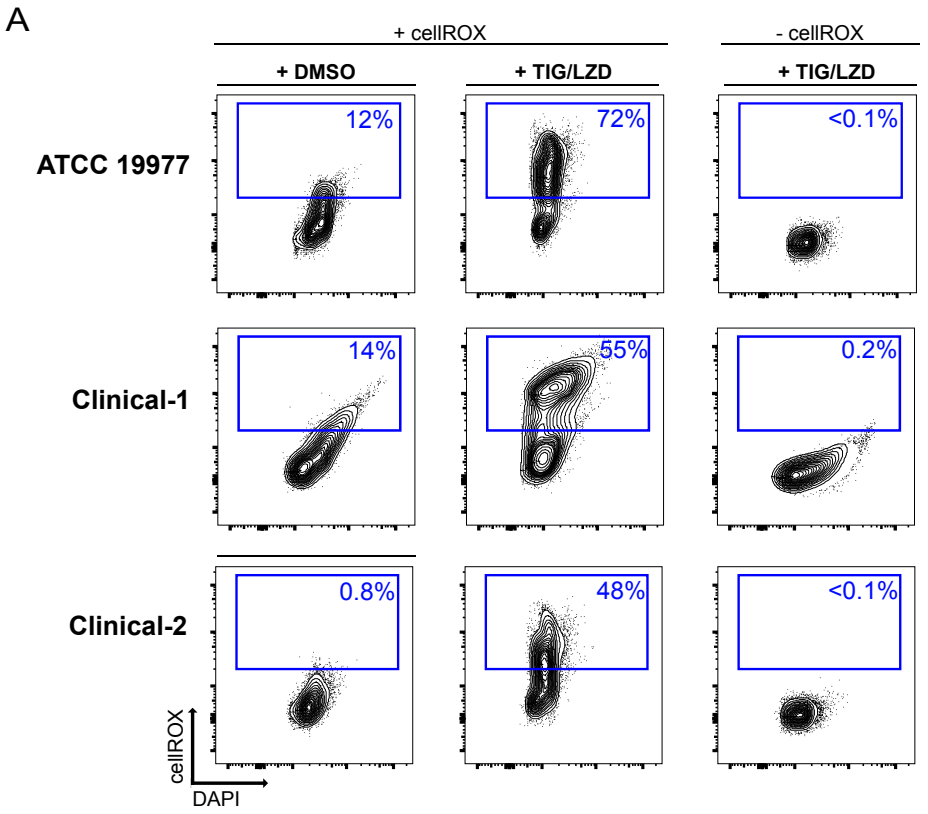
+ cellROX
- cellROX
+ DMSO
+ TIG/LZD
+ TIG/LZD
ATCC 19977
12%
72%
<0.1%
Clinical-1
14%
55%
0.2%
Clinical-2
0.8%
48%
<0.1%
cellROX
DAPI

B

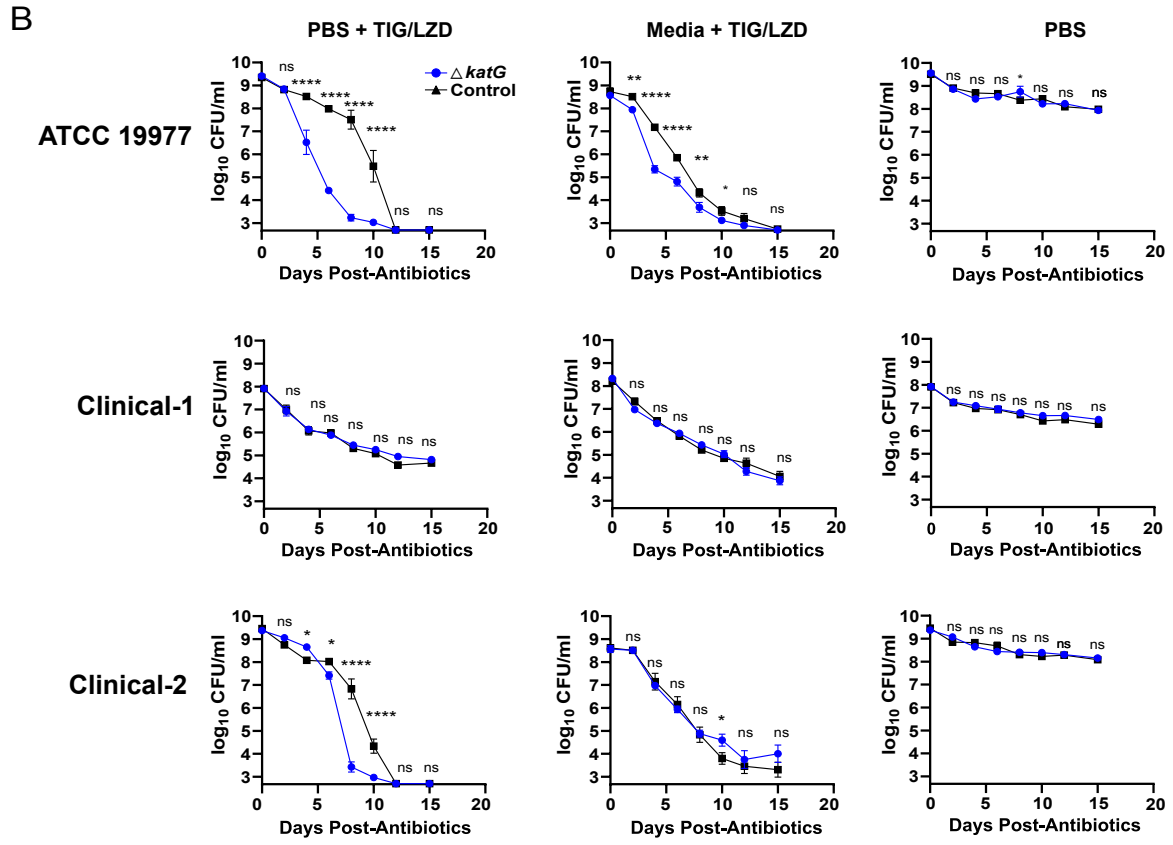
PBS + TIG/LZD
Media + TIG/LZD
PBS
ATCC 19977
Clinical-1
Clinical-2
△ katG
Control
log10 CFU/ml
Days Post-Antibiotics

FIGURE 3 - figure supplement 1

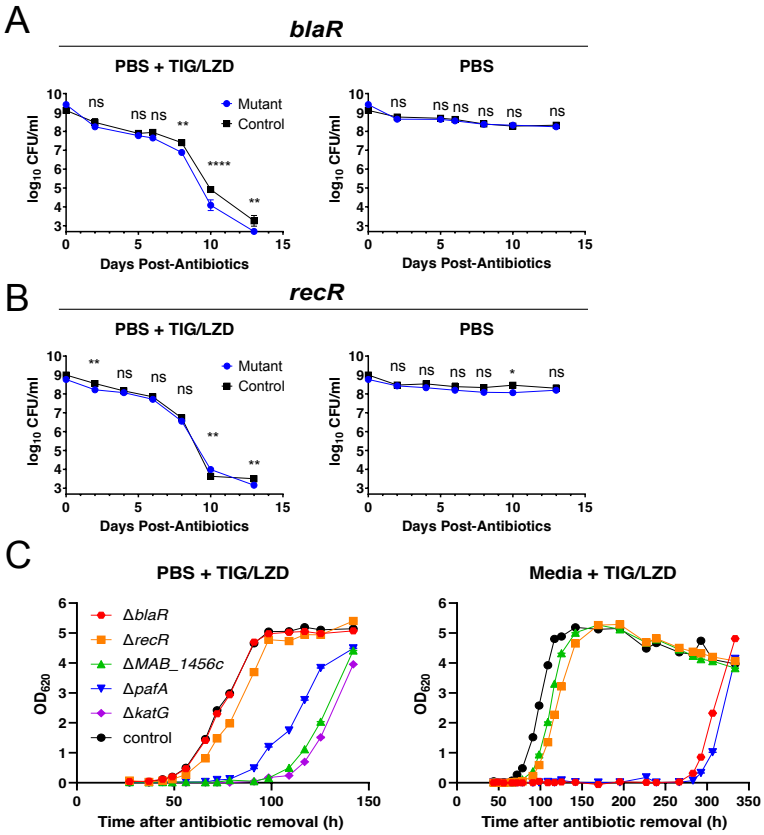
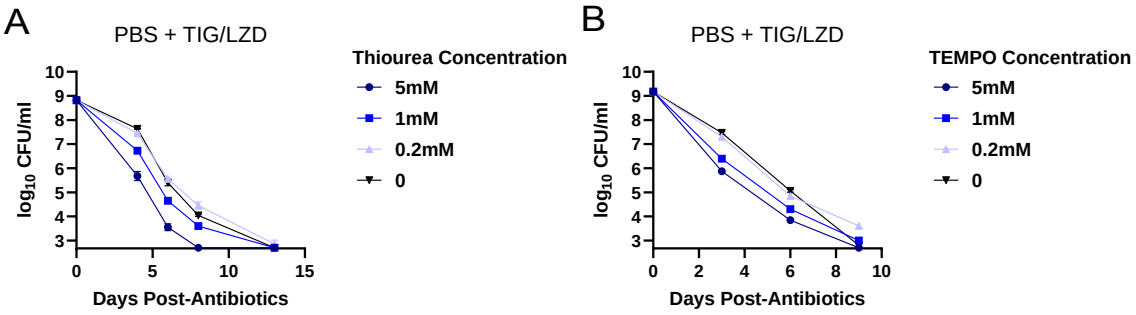
FIGURE 5 - figure supplement 1